GSI EMMI Hadron Physics Seminar
17. October 2018

A New QCD Facility at the CERN SPS M2 beam line

with a focus on
Proton radius measurement with high-energy muons
Hadron spectroscopy

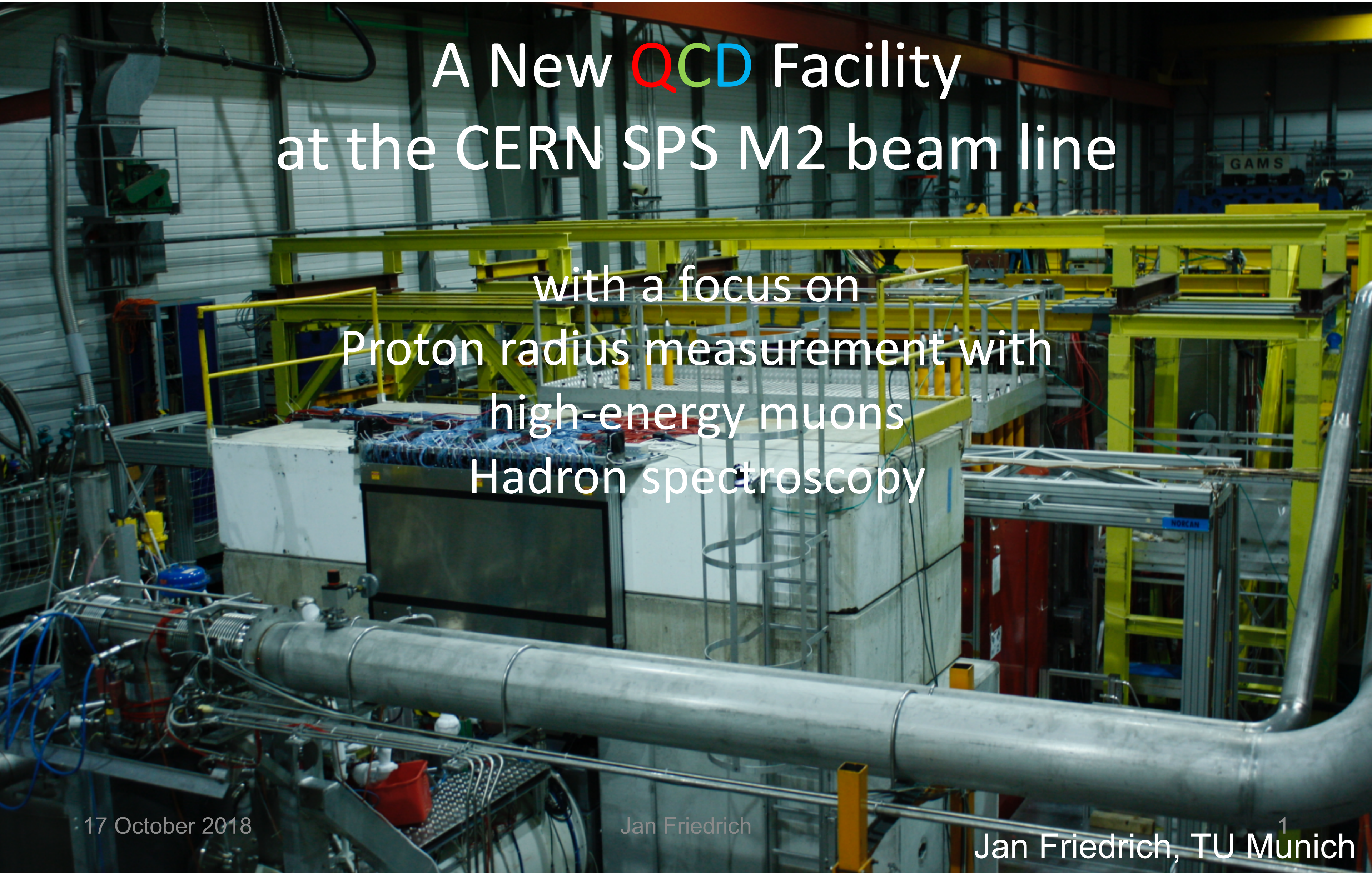

Jan Friedrich, TU Munich

Physics Case: Quantum Chromodynamics

Nucleons (and all hadrons) are made from Dirac particles (Quarks) bound by the color force (Gluons)

The properties of bound states are not calculable from first principles but need modelling

Important experimental input comes from lepton-hadron and hadron-hadron scattering

Many open questions (quark/gluon distributions/correlations, hadron sizes etc) need more experimental input

Letter of Intent for a New QCD Facility at CERN

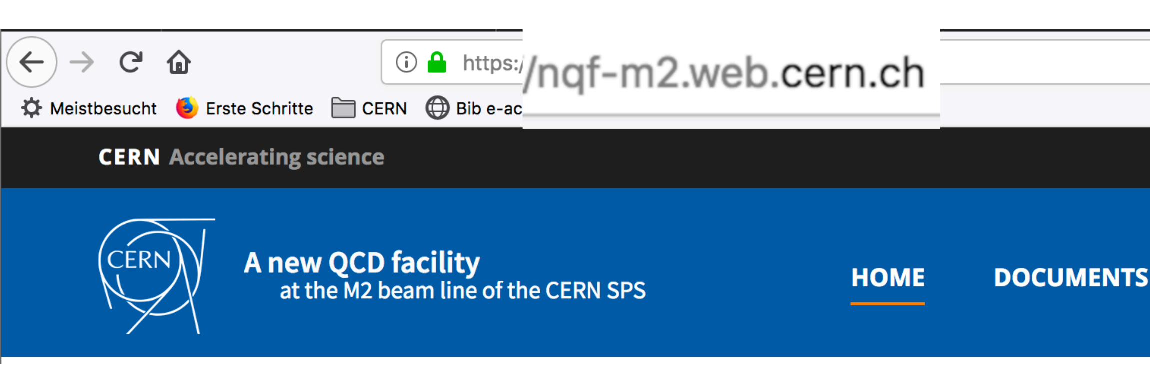

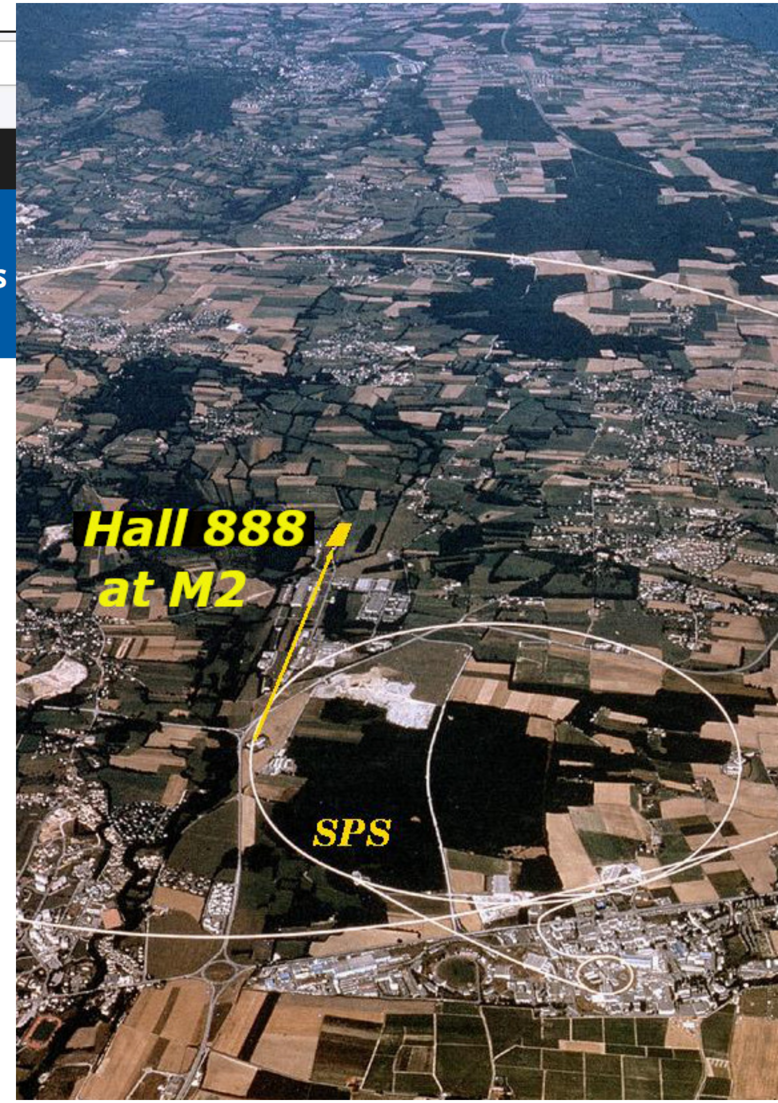

The M2 beam line of the CERN SPS has been built to deliver high-intensity muon beams to experiments in hall 888: EMC (1973), NMC, SMC, COMPASS (also „conventional“ hadron beams)

Idea for a follow-up apparatus: Letter of Intent

not a single experiment but a facility that bundles the needs of several campaigns into a common effort

EUROPEAN ORGANIZATION FOR NUCLEAR RESEARCH

Letter of Intent (Draft 2.0)

A New QCD facility at the M2 beam line of the CERN SPS

Letter of Intent working group

Proton radius measurement using muon-proton elastic scattering
Hard exclusive reactions using a muon beam and a transversely polarised target
Drell-Yan and charmonium production
Measurement of antiproton production cross sections for Dark Matter Search
Spectroscopy with low-energy antiprotons
Spectroscopy of kaons
Study of the gluon distribution in the kaon via prompt-photon production
Low-energy tests of QCD using Primakoff reactions
Production of vector mesons and excited kaons off nuclei

COMPASS QCD facility at CERN (SPS)

COmmon Muon Proton Apparatus for Structure and Spectroscopy

~240 physicists, 12 countries + CERN, 24 institutions

Reminder of the COMPASS physics program

COMPASS

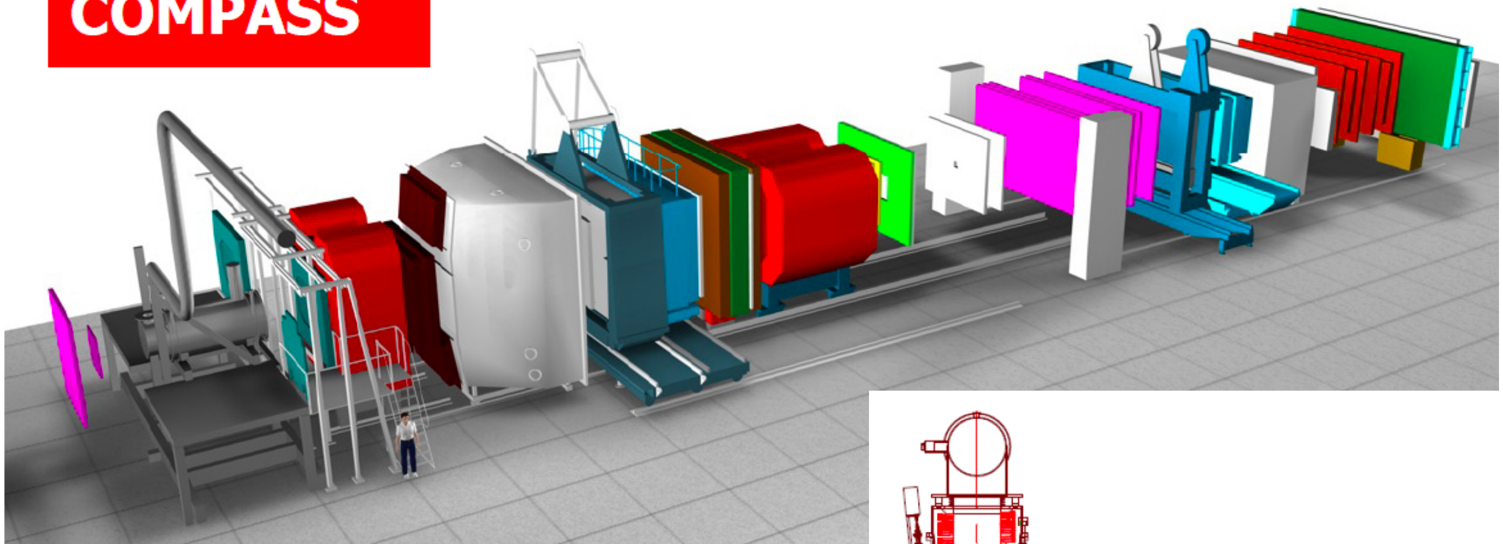

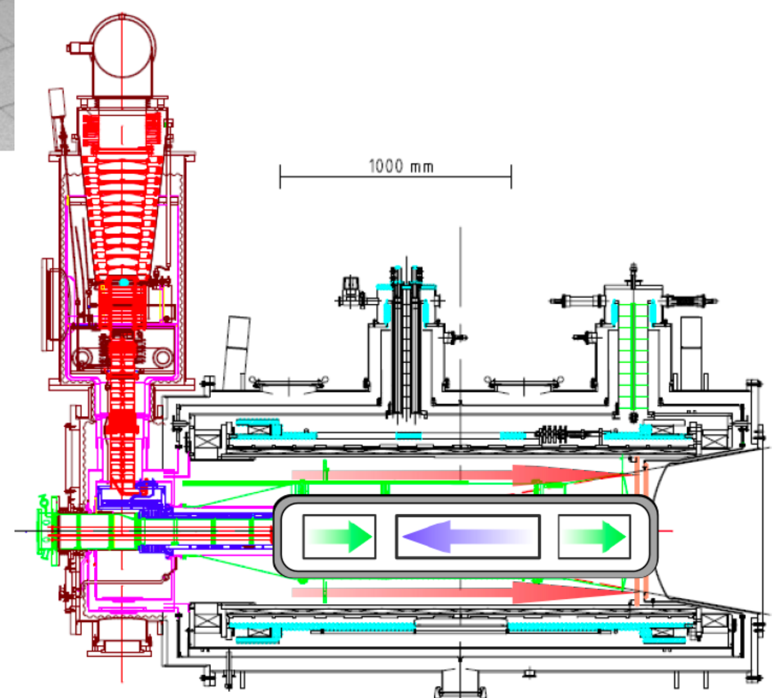

Versatile apparatus to investigate QCD:
Two-stage COMPASS Spectrometer

1. Muon, electron and hadron beams with momenta 20-250 GeV and intensities up to 10^8 particles per second
2. Solid-state polarised (NH_3 or ^{6}LiD), liquid hydrogen and nuclear targets
3. Powerful tracking (350 planes) and PID systems (Muon Walls, Calorimeters, RICH)

COMPASS QCD facility at SPS M2 beam line (CERN) secondary hadron and lepton beams

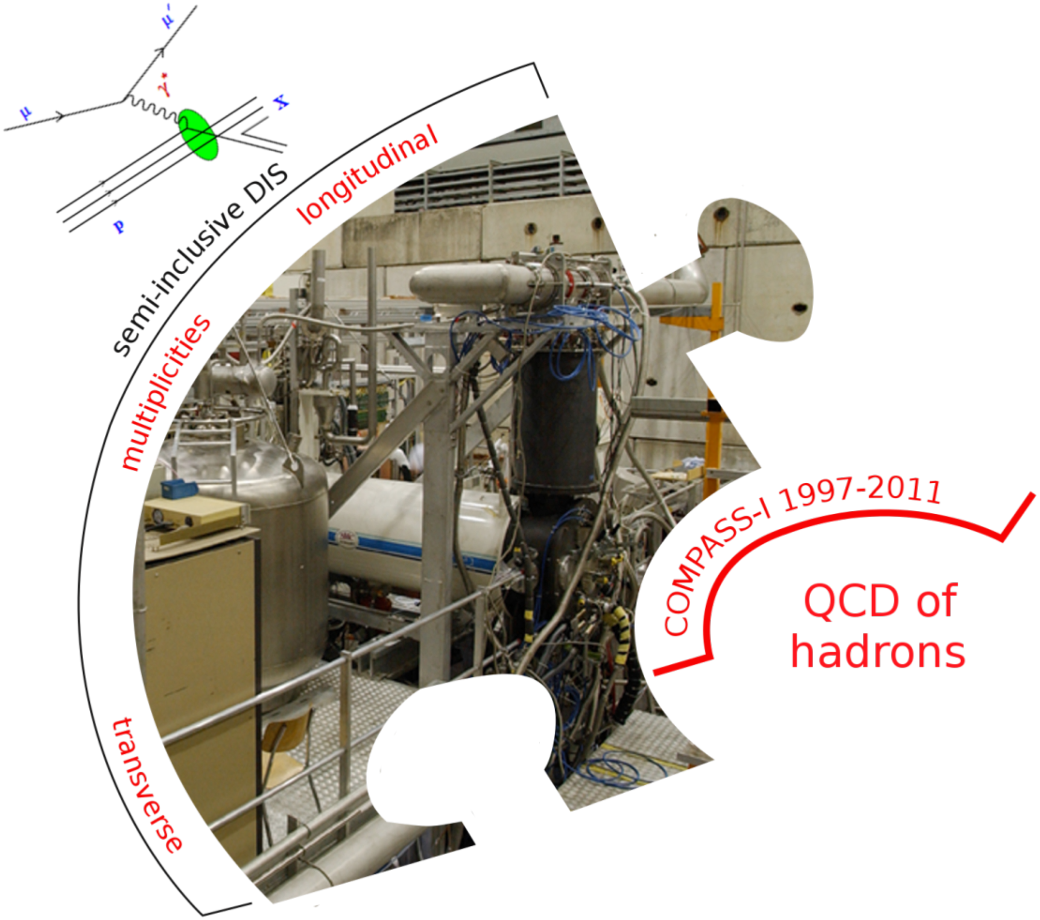

COMPASS QCD facility at SPS M2 beam line (CERN) secondary hadron and lepton beams

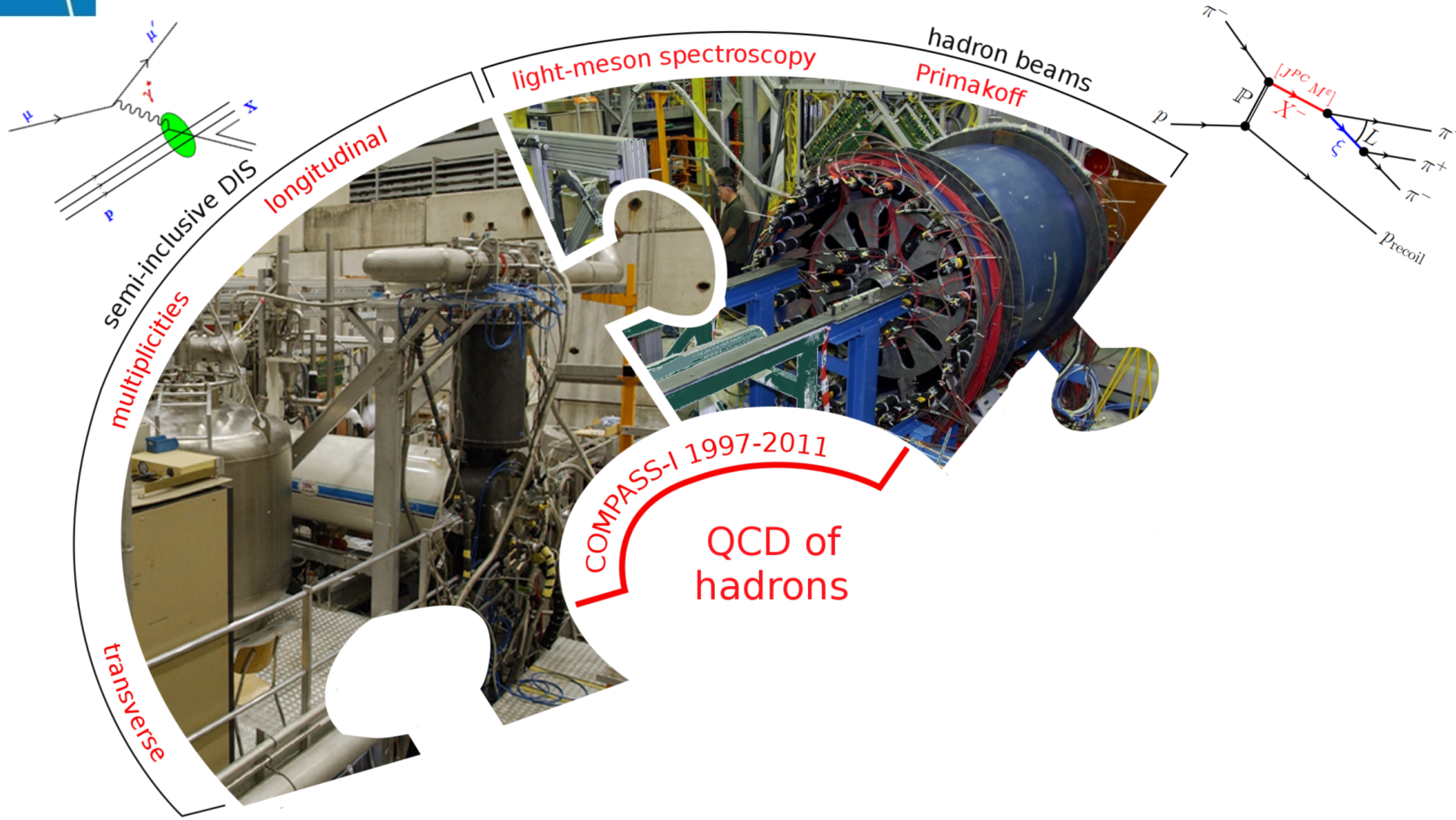

COMPASS QCD facility at SPS M2 beam line (CERN) secondary hadron and lepton beams

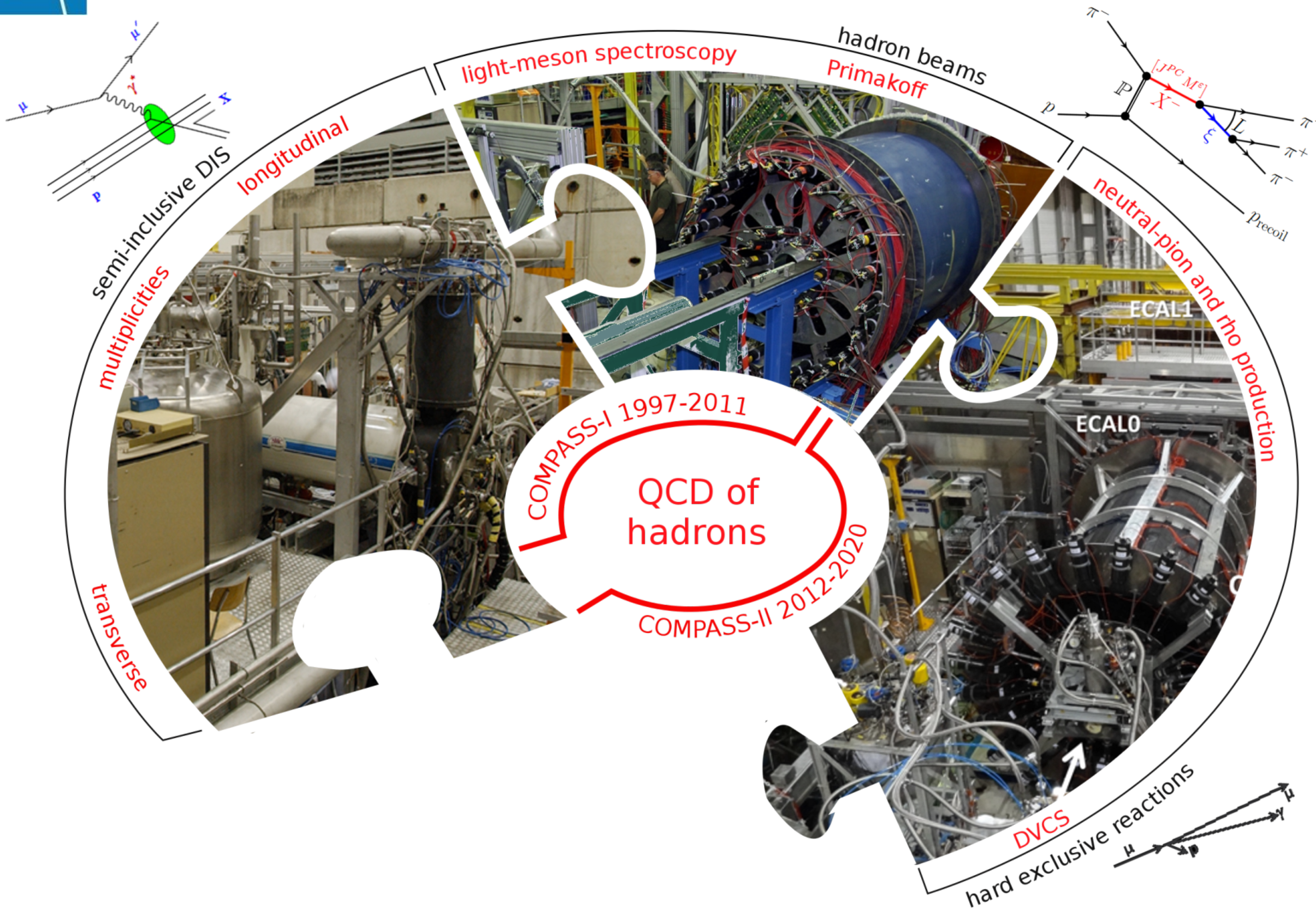

COMPASS QCD facility at SPS M2 beam line (CERN) secondary hadron and lepton beams

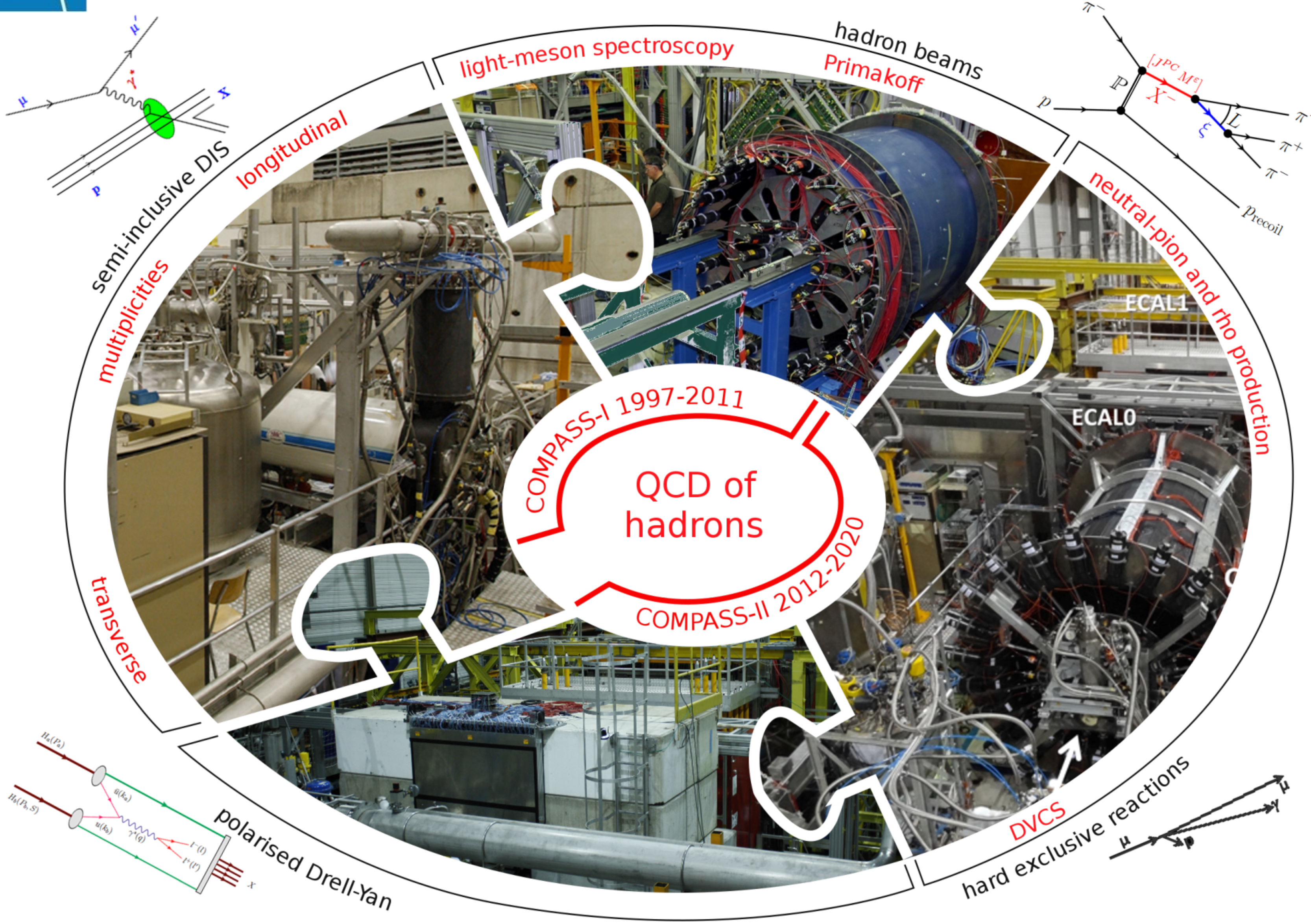

COMPASS QCD facility at SPS M2 beam line (CERN) secondary hadron and lepton beams

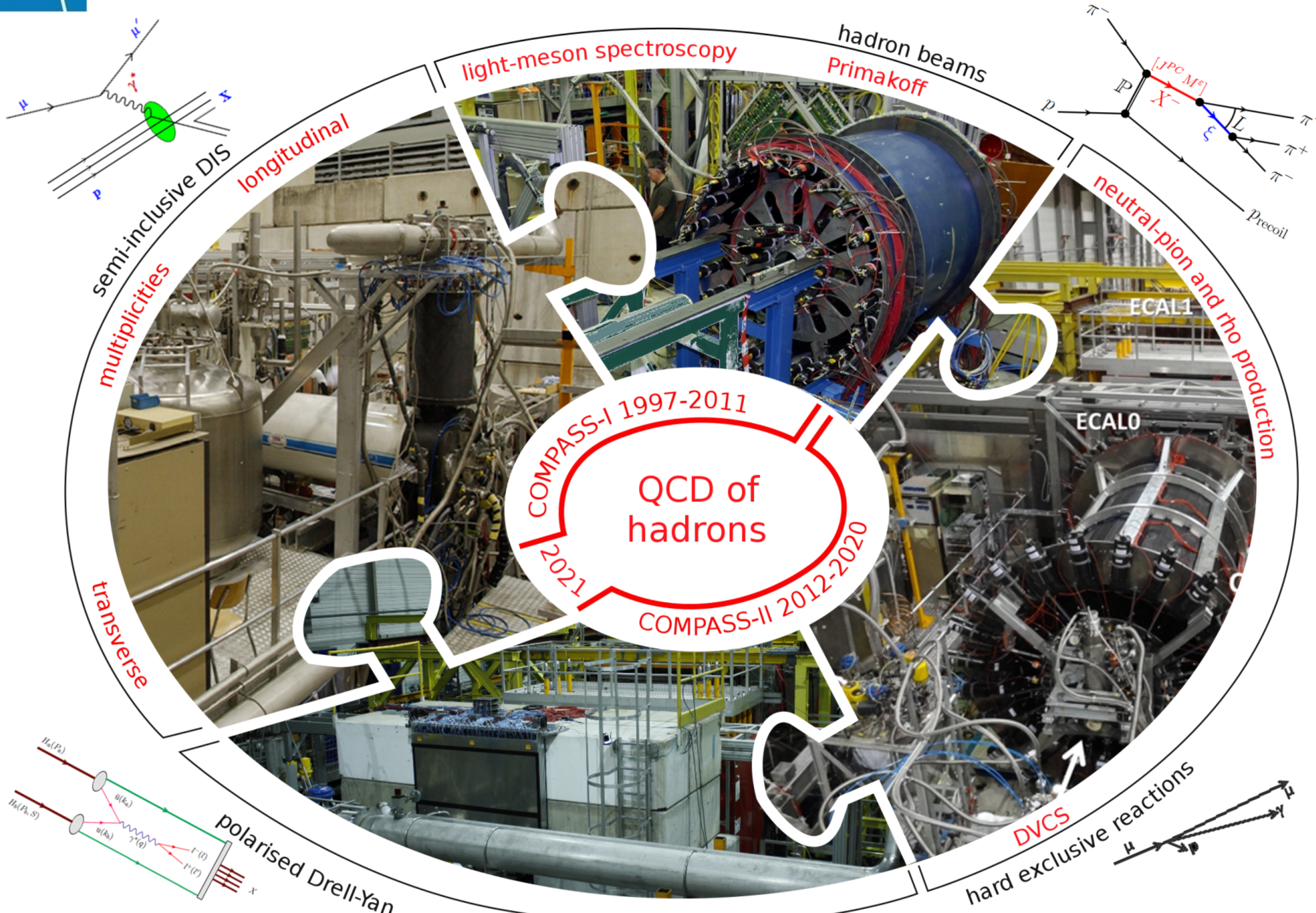

Proton radius and form factors

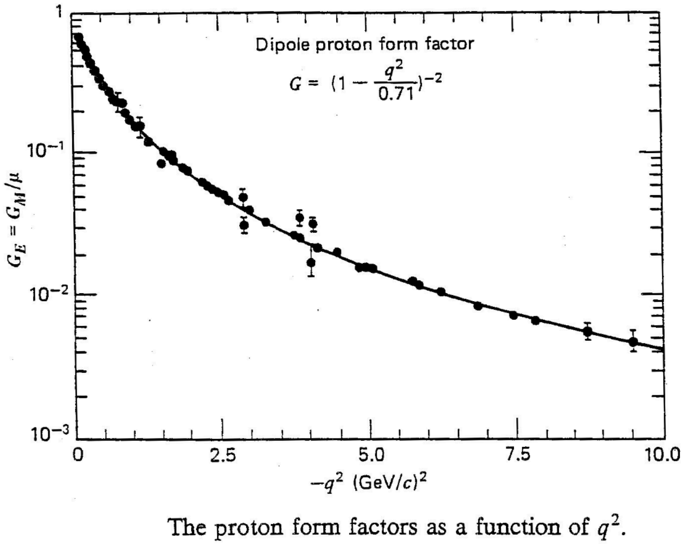

The proton form factors as a function of q^2.

← Fourier → transform

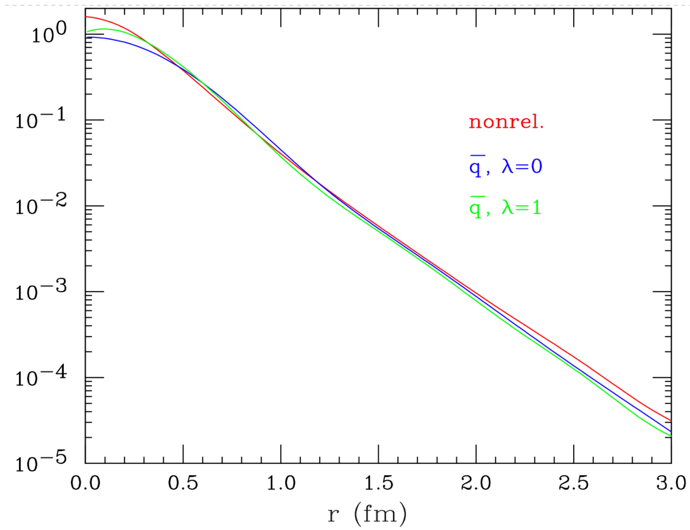

I. Sick 2006

The proton form factors are measured in elastic lepton-proton scattering.

The finite-size effect also enters in the splitting of (exotic) atom levels measured in laser spectroscopy

$$\langle r_E^2 \rangle = -6\hbar^2 \frac{dG_E(Q^2)}{dQ^2}\Big|_{Q^2 \to 0}$$

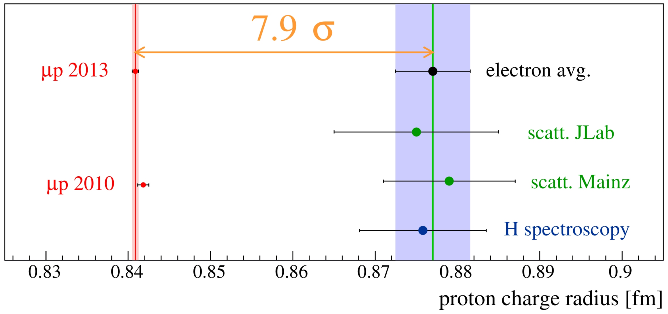

Proton radius puzzle:
without H spectroscopy ~5σ

Proton radius:

Discrepancy in terms of form factor slope

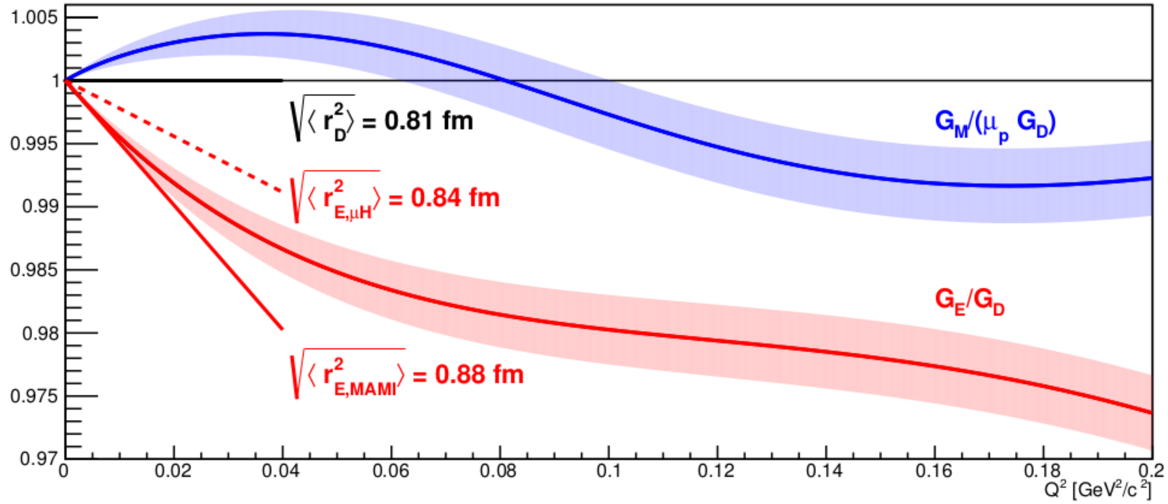

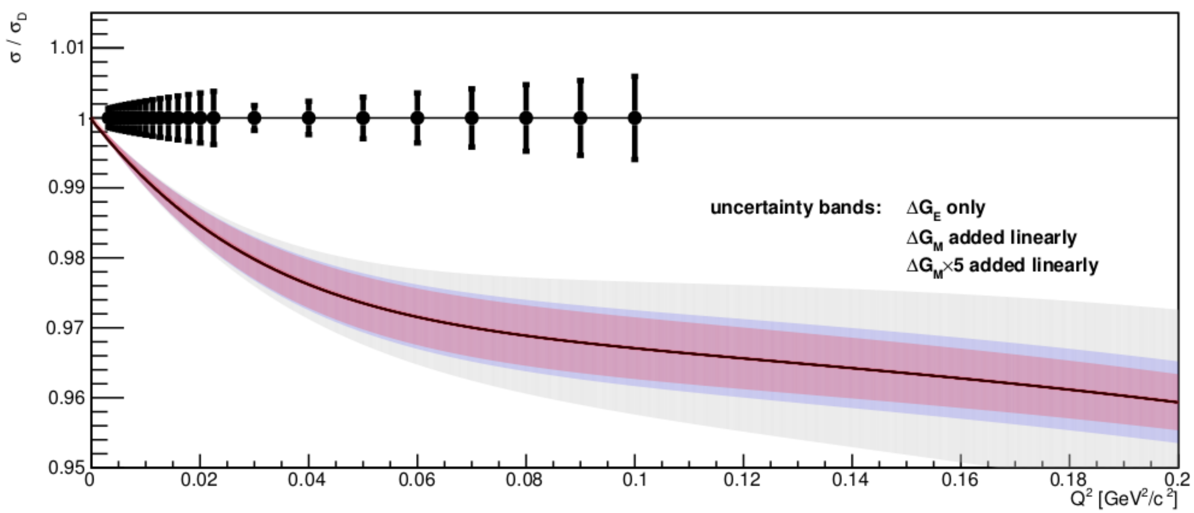

Why high-energy muons?

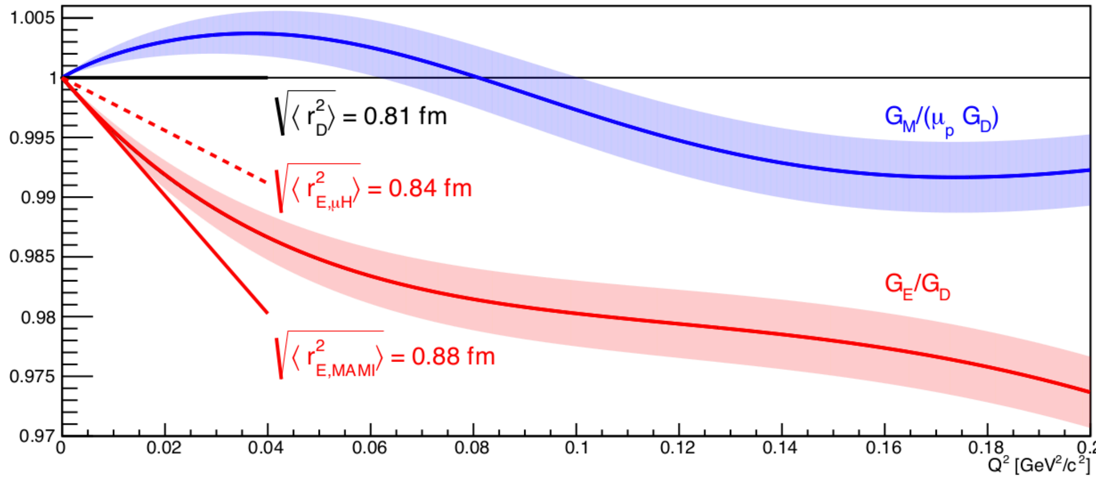

opportunity for new generation experiment at M2 beam line

- scatter muon beam off proton target
- measure cross-section dependence on Q^2
- obtain combination of electric and magnetic form factor $G_E^2 + \tau G_M^2$
  - form factors cannot be separated due to high beam energy
- compared to e^- beam: smaller radiative corrections
- compared to μ beam at low energies: smaller Coulomb corrections

Why high-energy muons?

QED radiative corrections

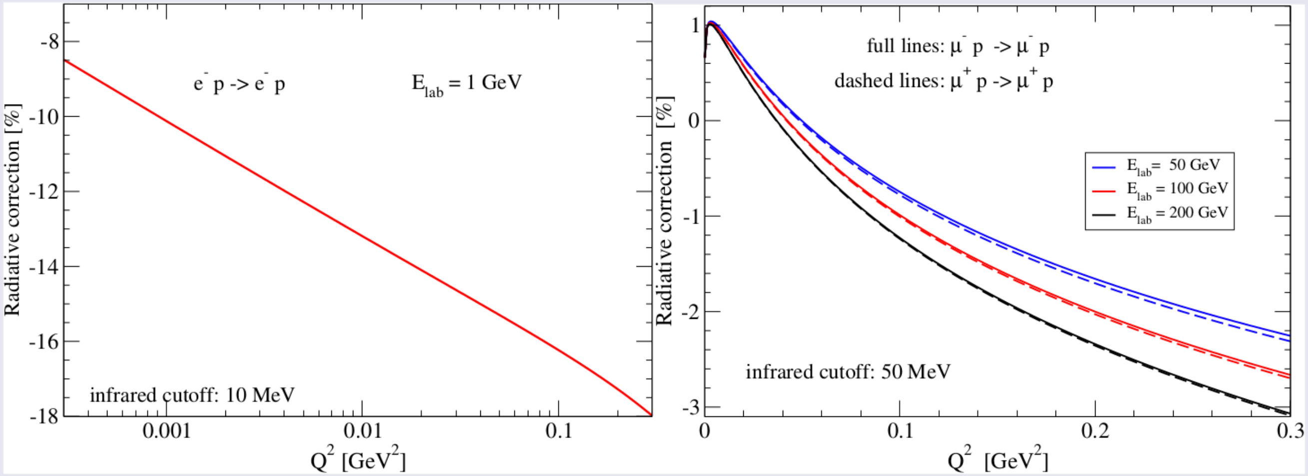

- for soft bremsstrahlung photon energies ($E_\gamma / E_{beam} \sim 0.01$), QED radiative corrections amount to $\sim$ 15-20% for electrons, and to $\sim$ 1.5% for muons
- important contribution to the uncertainty of elastic scattering intensities: *change* of this correction over the kinematic range of interest
- check: impact of exponantiation procedure (stricty valid only for vanishing photon energies): e^-: $2 - 4\%$, μ^-: 0.1%
- integrating the radiative tail out to large fraction of beam energy: shifts the correction to smaller values, but only *increases* the uncertainty

Proton radius measurement at CERN

General idea: measure the proton form factor slope using the high-energy muon beam on a high-pressure hydrogen target

In a one-year measurement, we estimate to achieve a precision of ~0.01fm on the proton radius, thus contribute to resolve the proton radius puzzle between
  0.84 fm (muonic hydrogen laser spectroscopy)
  0.88 fm (electron scattering)

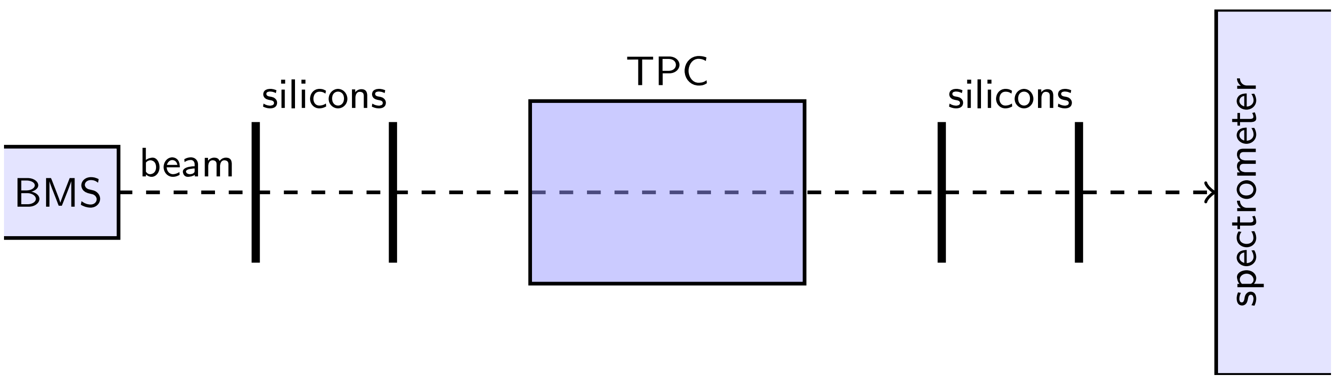

trigger concepts under study:
 triggerless readout (for 2e6…2e7/s)
 kink trigger (for Q^2 >3e-4)

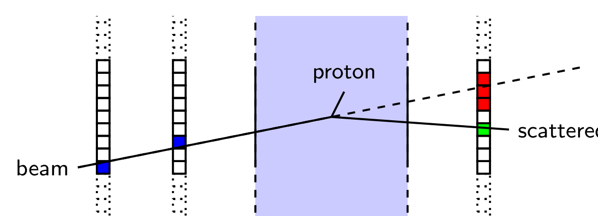

A new TPC

- high-pressure hydrogen target 4-20 bar
- measurement of recoil proton
- wide range of recoil energies 0.5 – 100 MeV
- required energy resolution ~60 keV

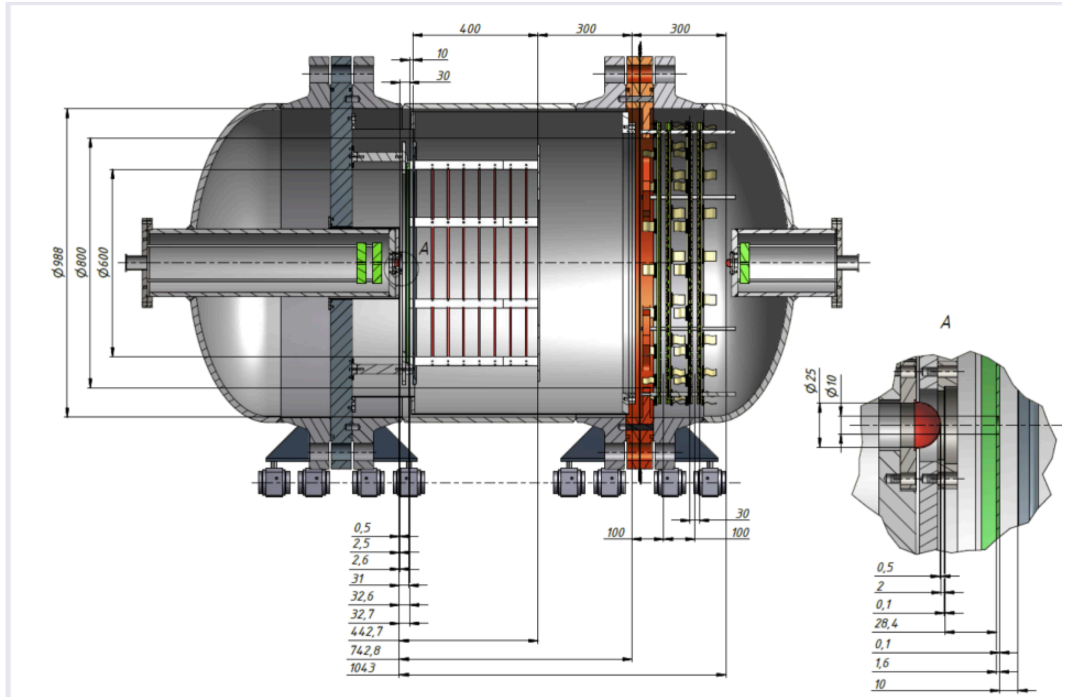

A new dedicated TPC for the experiment at CERN is being developed, ATTRACT application for European research funding (GSI/TUM) , in view of a possible later usage at FAIR R3B

Test Measurement in 2018

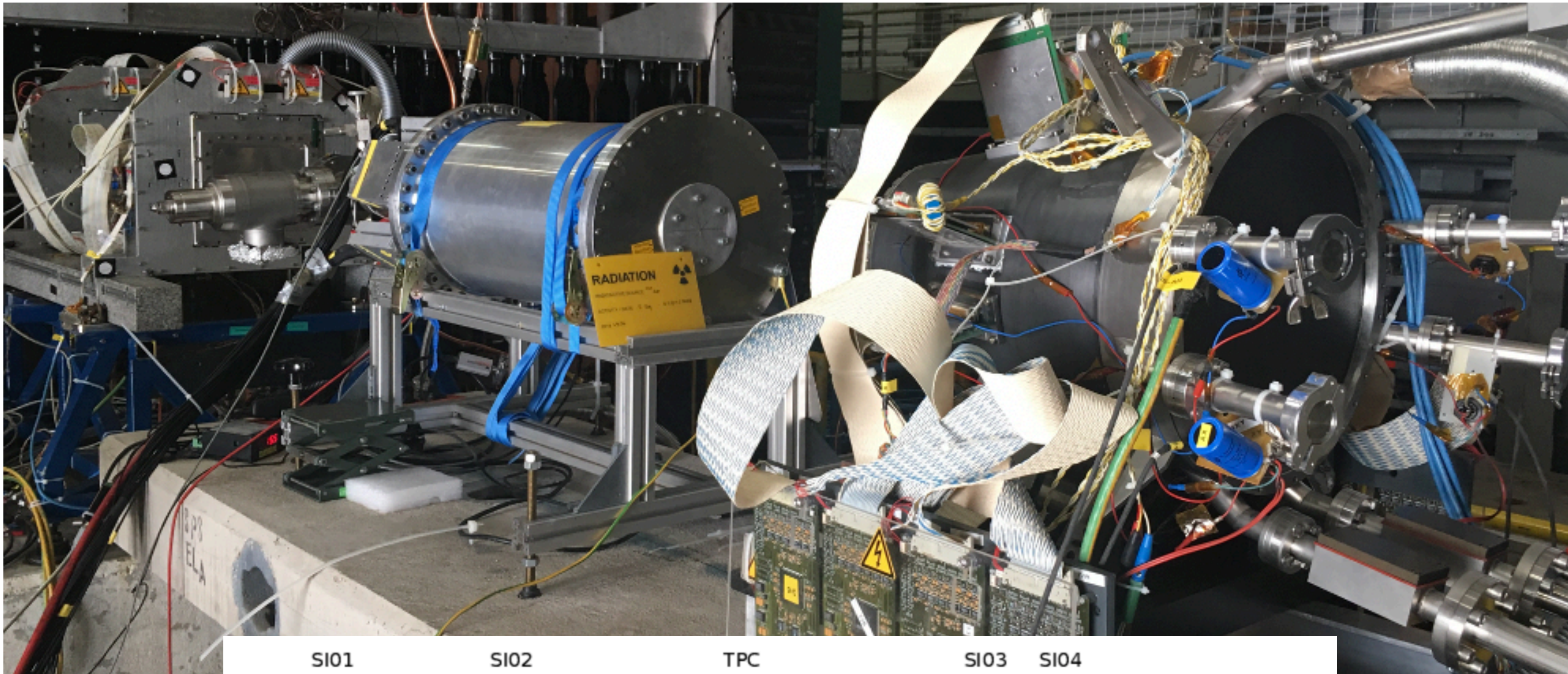

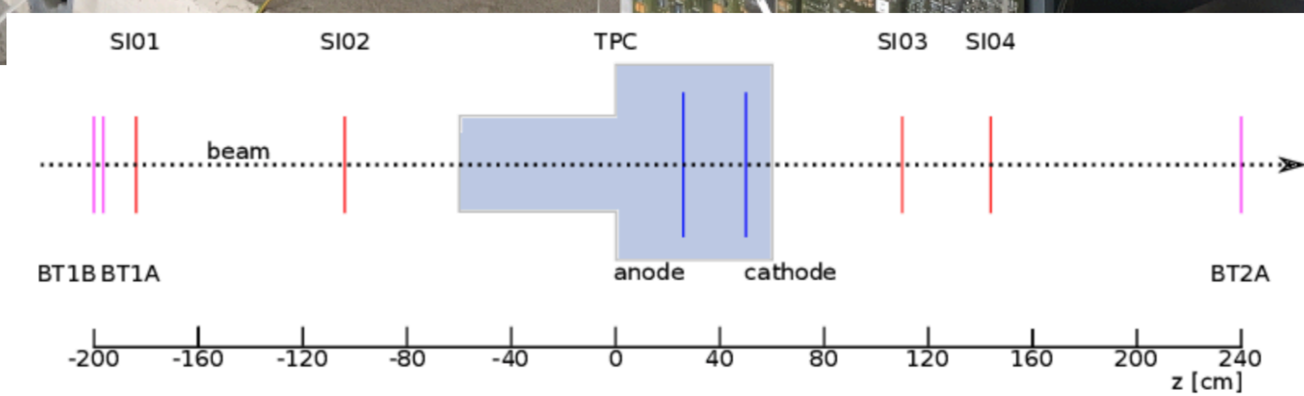

Proton radius test measurement: Vertex position (silicon detectors)

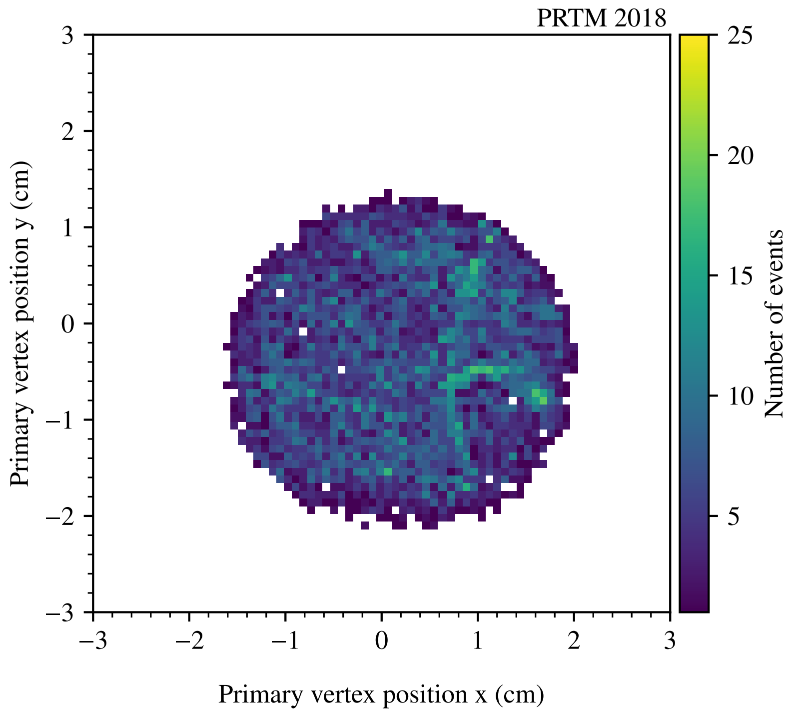

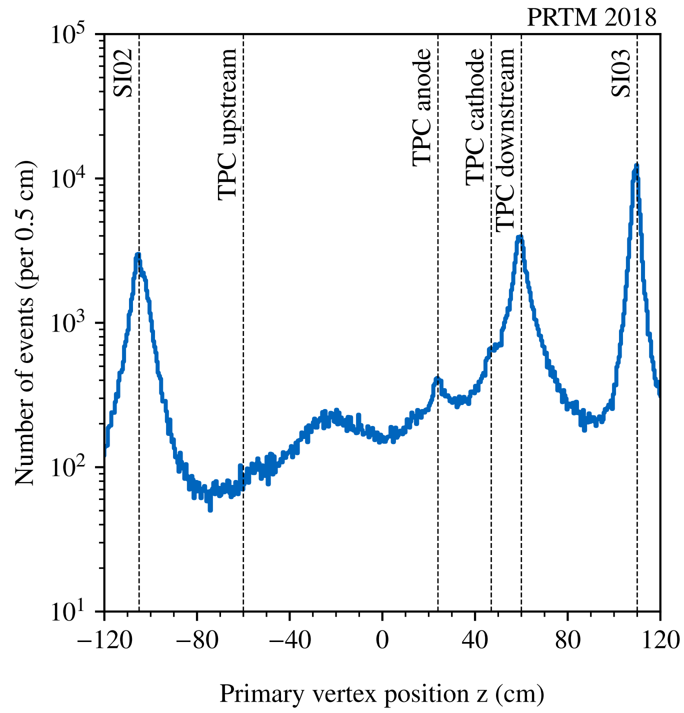

Combined information from TPC and silicons

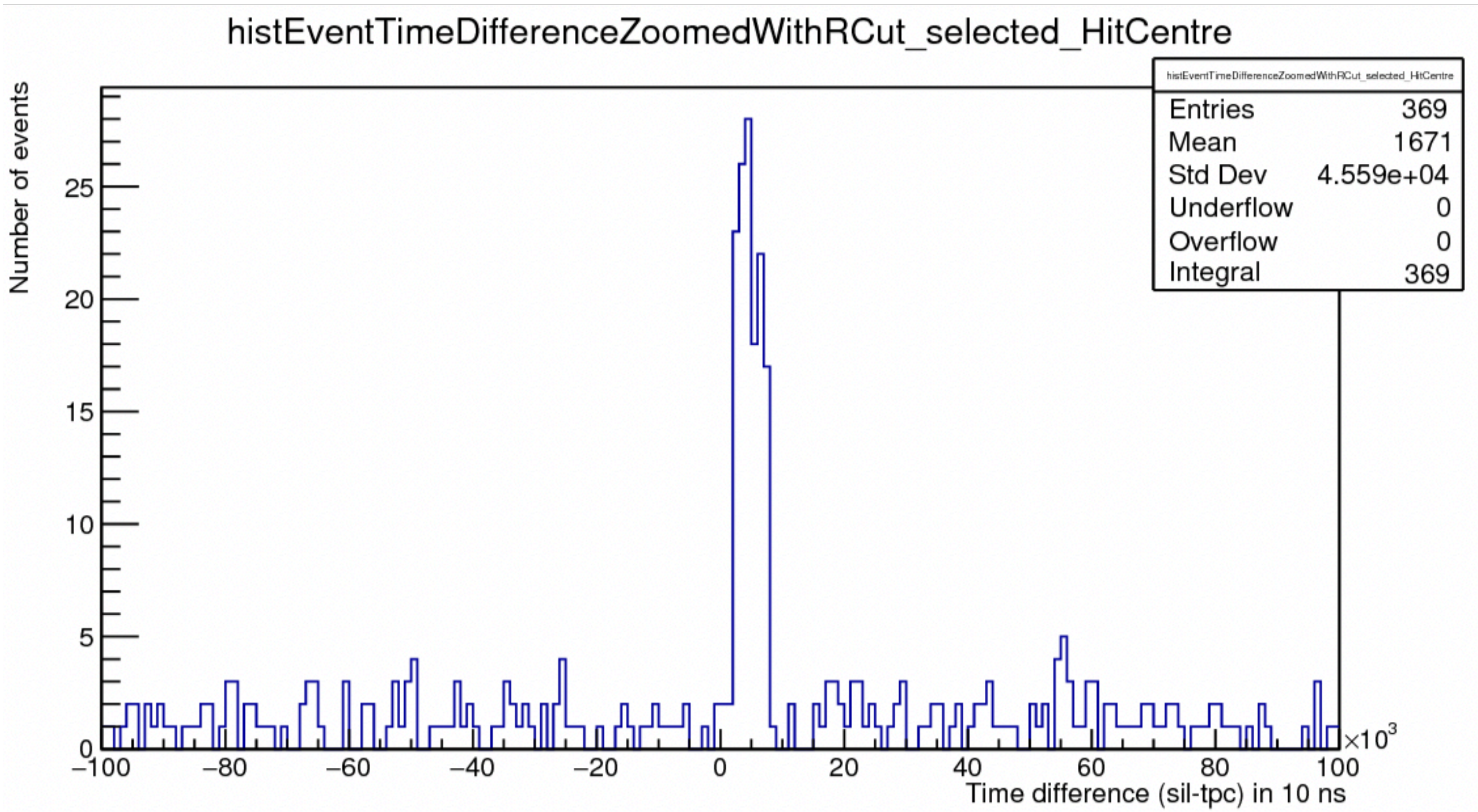

recording by 2 independent DAQ systems for TPC and silicon detectors
→ reading of a common „speaking clock" as time reference
(ongoing analysis)

Other topics with „conventional beams"

- muon beam
  - proton radius: on high-pressure TPC
  - DVCS on a transversely polarized target: recoil (silicon) detector to be inserted in the cold volume of the target magnet

- hadron beams
  - Drell-Yan and charmonium production with the π^-, K^-, p-bar and the π^+, K^+, p beams
  - antiproton production through p beam
  - antiproton spectroscopy: lower-energetic (<20GeV) negative beam contains large fraction of antiprotons: p-bar annihiliation can be used for X,Y,Z spectroscopy at luminosity 10^{30} cm^{-2} s^{-1}
    → preparational step for PANDA?

A new beamline: radio-frequency separation of hadron beams

Reminder: Panofsky-Schnell-System with two cavities (CERN 68-29)

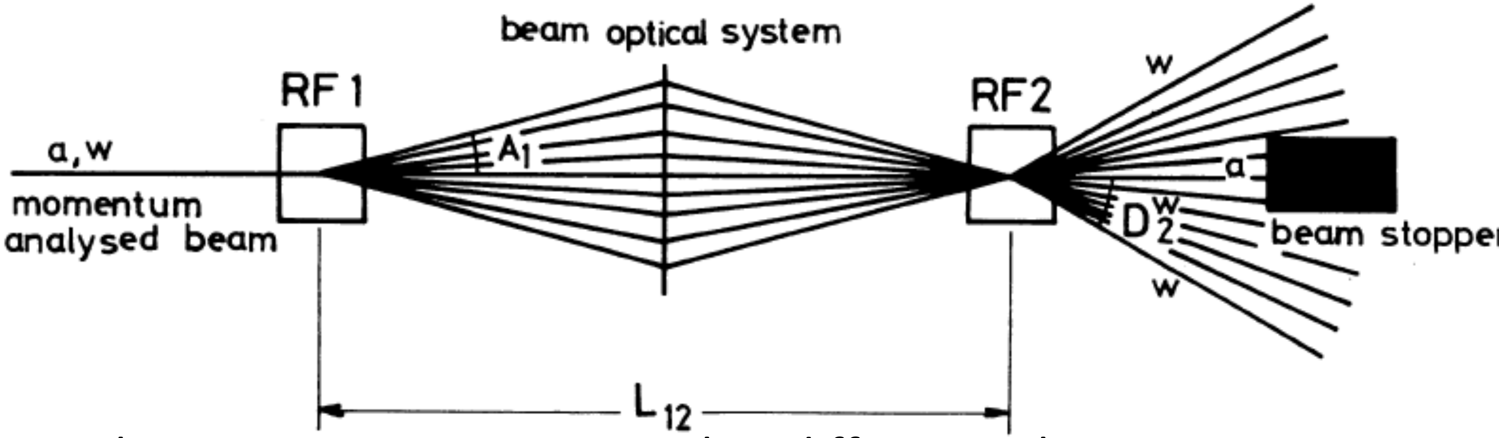

- Particle species: same momenta but different velocities
- Time-dependent transverse kick by RF cavities in dipole mode
- RF1 kick compensated or amplified by RF2
- Selection of particle species by selection of phase difference
  $\Delta\Phi = 2\pi\,(L\,f\,/\,c)\,(\beta_1^{-1} - \beta_2^{-1})$
- For large momenta: $\beta_1^{-1} - \beta_2^{-1} = (m_1^2 - m_2^2)/2\mathbf{p}^2$

Physics with RF-separated K beams

- Drell-Yan process with kaons: partonic structure of K

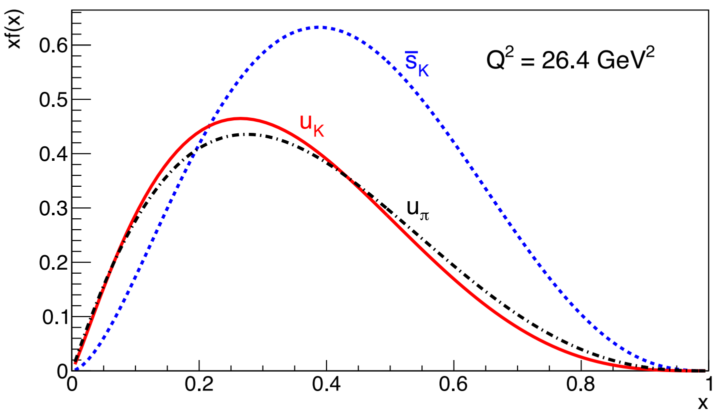

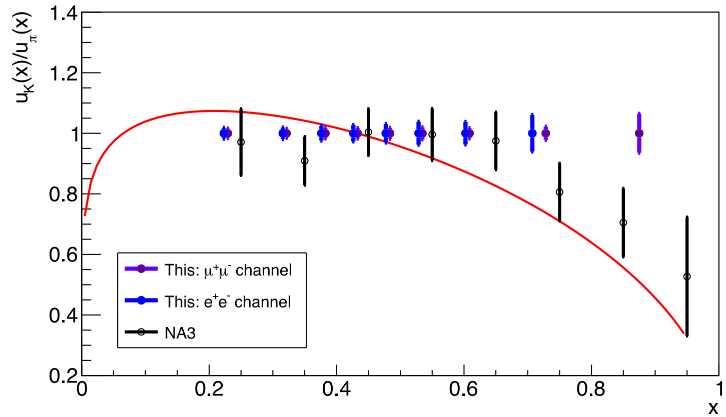

- Kaonic excitation spectrum in diffractive dissociation of a kaon beam

Physics with hadron beams:
COMPASS main results

PHYSICAL REVIEW D **95**, 032004 (2017)

Resonance production and $\pi\pi$ S-wave in $\pi^- + p \to \pi^-\pi^-\pi^+ + p_{\mathrm{recoil}}$ at 190 GeV/c

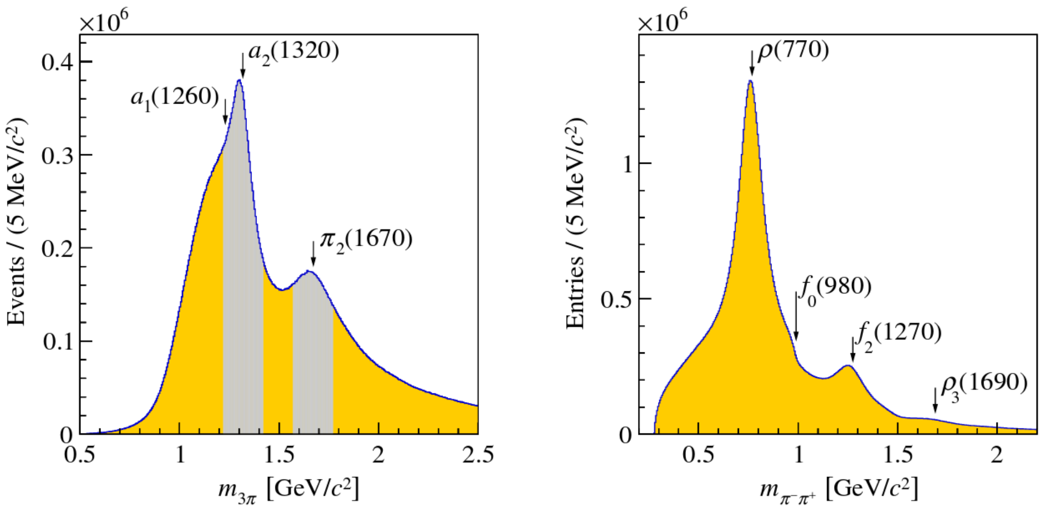

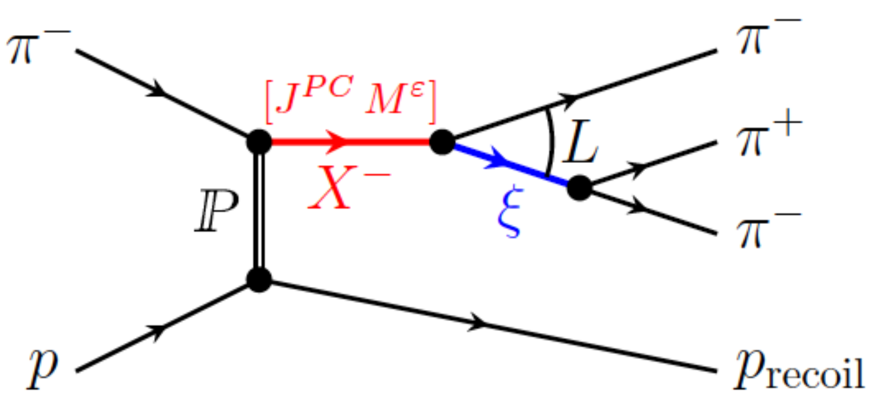

published in 2017: PRD 59 pages

2008-2009 data taking, 190 GeV/c hadron beam on a hydrogen target

3π data sample ~50 million events
10x to 100x previous experiments
allows for fine binning in masses and momentum transfer

partial-wave analysis in *3π*-mass slices, detailed understanding of the *2π*-isobars

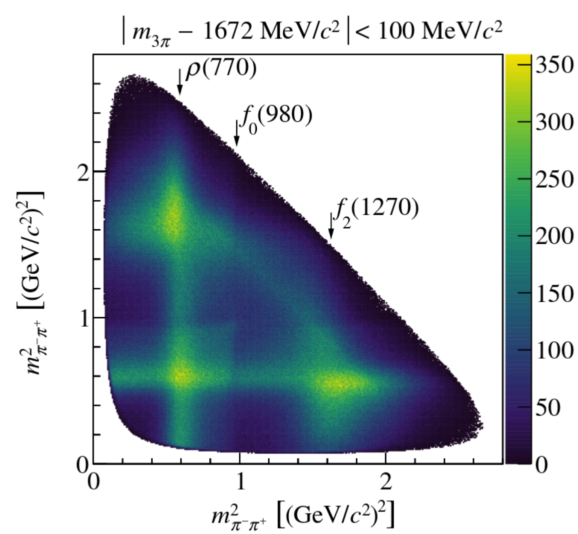

Physics with hadron beams: meson spectroscopy

main results

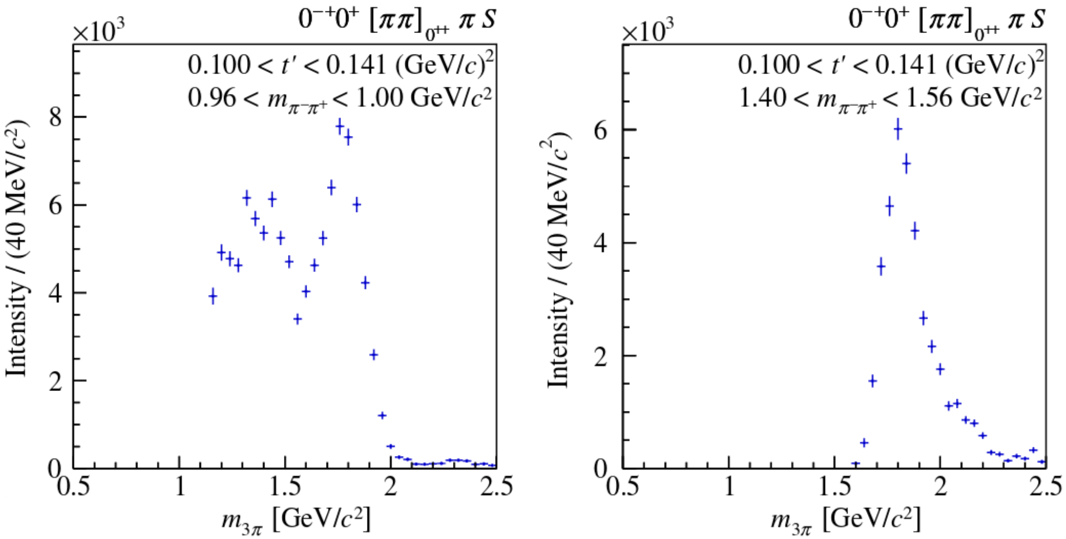

example: partial wave for *π(1800)*

investigation of 2π isobar structure reveals contributions from $f_0(980)$ and $f_0(1500)$

recently accepted: paper on partial-wave fits including 3π resonances, PRD 75 pages

Light isovector resonances in $\pi^- p \to \pi^-\pi^-\pi^+ p$ at 190 GeV/c

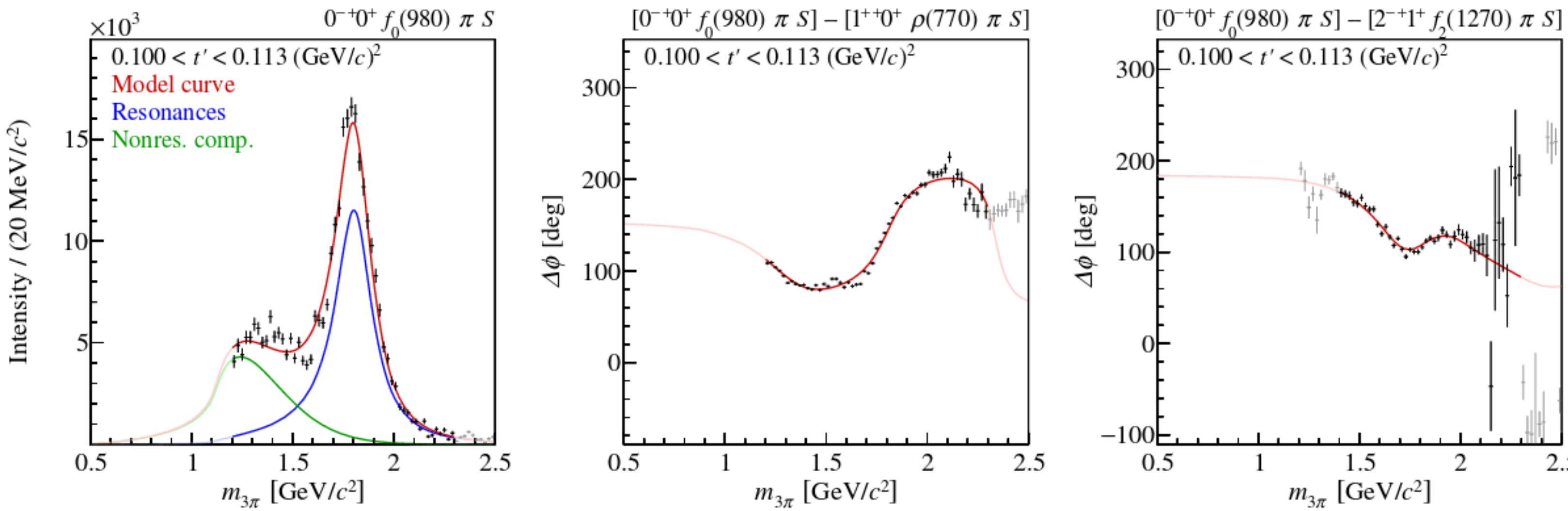

Physics with hadron beams: meson spectroscopy
main results

Light isovector resonances in $\pi^- p \rightarrow \pi^- \pi^- \pi^+ p$ at 190 GeV/c

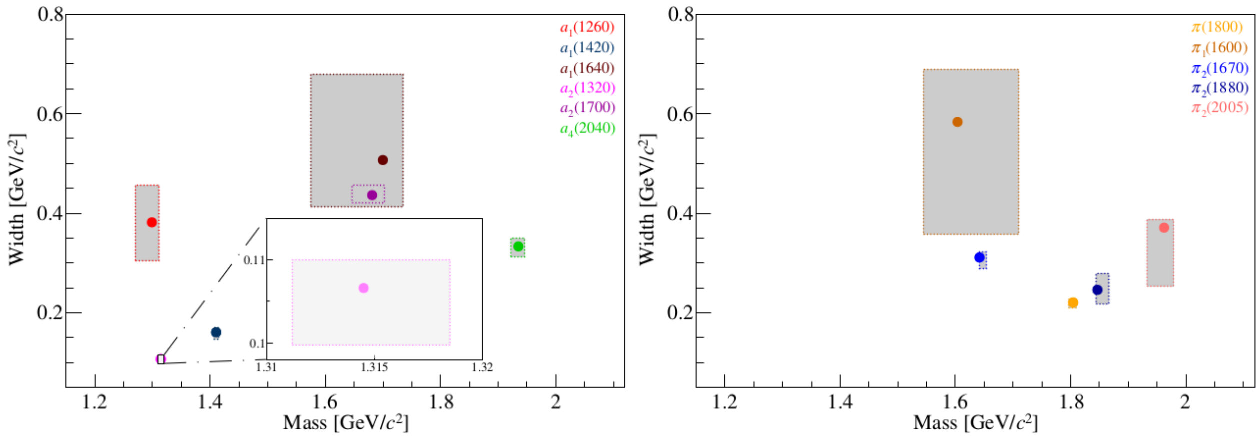

resonance parameters with unprecedented precision and systematic investigations:
6 a-like and 5 π-like states

broad spin-exotic $\pi_1(1600)$

further investigations of the $a_1(1420)$ found by COMPASS: triangle amplitude consistent with Breit-Wigner

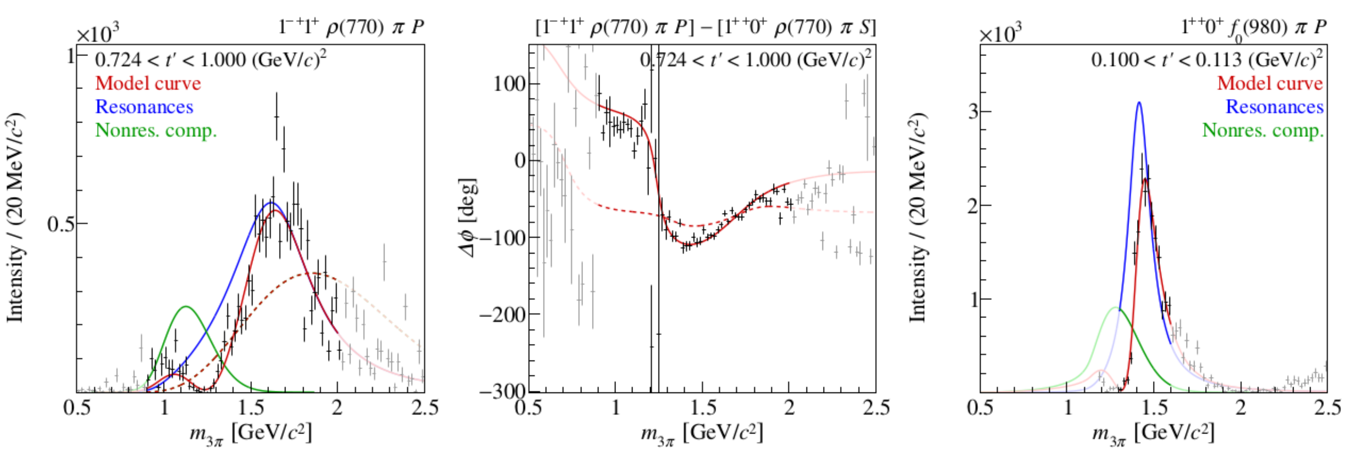

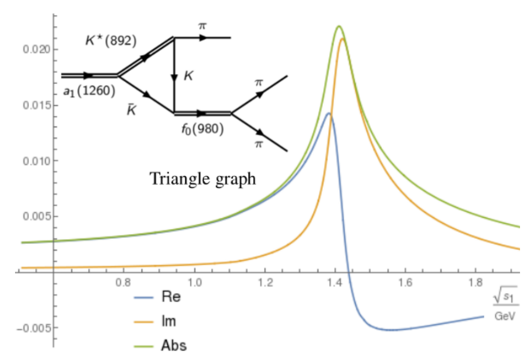

Kaon excitation spectrum

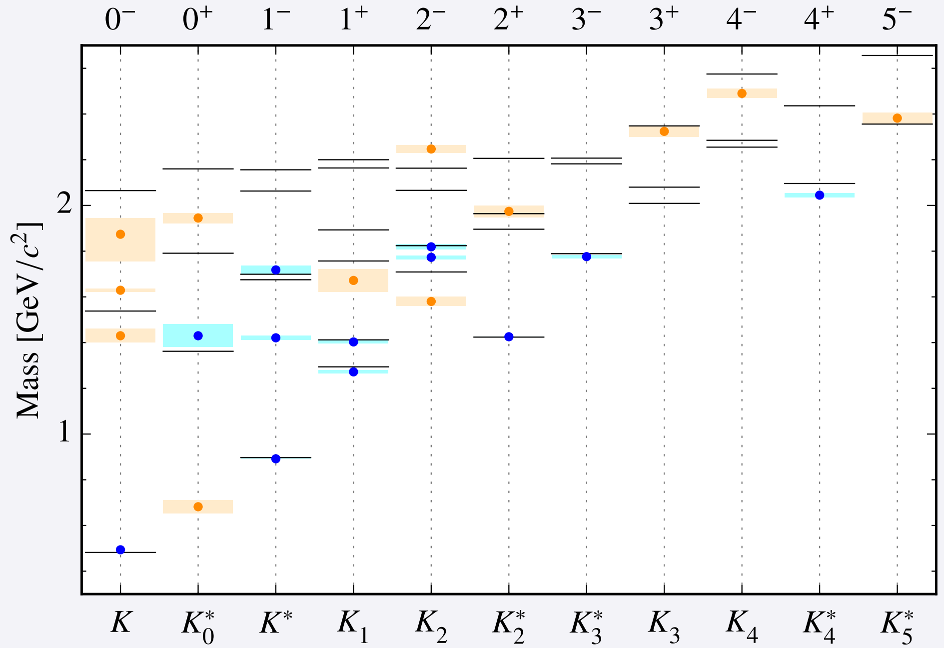

[Courtesy of S. Wallner, TUM]

- 25 kaon states listed by PDG (<3.1GeV), 13 of those need confirmation
- many predicted quark-model states still missing
- some hints for supernumerous states

New data with RF-separated K beam

- Kaon content of negatively charged 190 GeV hadron beam: 2% (pions 97%), currently at COMPASS allowed 10^5 K/s
- Intensity can be increased by factor 10 if beam is RF-separated
- corresponds to > 10^7 $K^- \pi^+ \pi^-$ events, approx. 10x world data
- Competition: J-PARC K^- beams (2-10 GeV → more complicated production mechanism, smaller CM energy), GlueX at Jlab (K_L beam, main focus hyperon spectroscopy, Phase IV photon beams, kaon excitations in subsystems, difficult analysis), τ lepton decays at BESIII, Belle2, LHCb
- needed (upgraded) detector components: CEDAR detectors (beam PID) with increased stability and rate capability, improved target proton recoil detector, final-state PID: RICH detector covers the range10-50 GeV, add RICH0 for smaller momenta?

Timelines

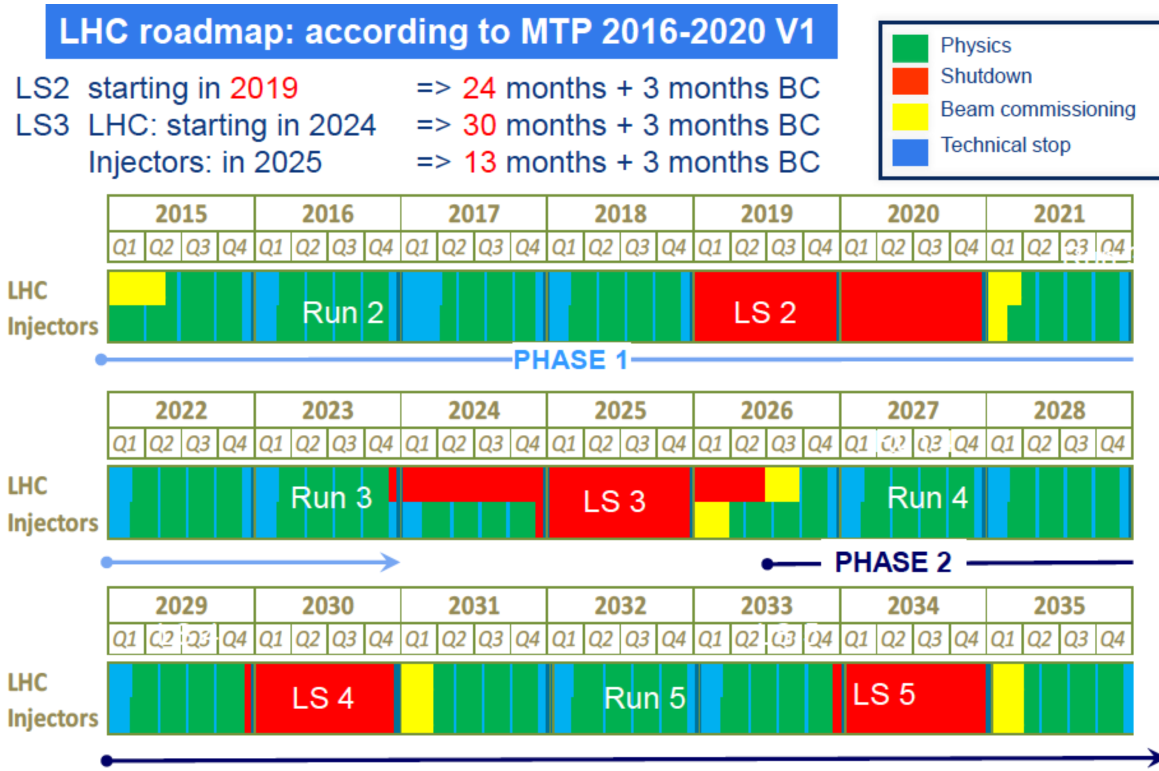

- conventional-beams program: 2022-2024
- RF-separated beams: from 2026 on

Summary of Physics

Program	Physics Goals	Beam Energy [GeV]	Beam Intensity [s^{-1}]	Trigger Rate [kHz]	Beam Type	Target	Earliest start time, duration	Hardware additions
muon-proton elastic scattering	Precision proton-radius measurement	100	$4 \cdot 10^6$	100	$\mu^\pm$	high-pressure H2	2022 1 year	active TPC, SciFi trigger, silicon veto,
Hard exclusive reactions	GPD E	160	$2 \cdot 10^7$	10	$\mu^\pm$	$NH_3^\uparrow$	2022 2 years	recoil silicon, modified polarised target magnet
Input for Dark Matter Search	$\overline{p}$ production cross section	20-280	$5 \cdot 10^5$	25	p	LH2, LHe	2022 1 month	liquid helium target
$\overline{p}$-induced spectroscopy	Heavy quark exotics	12, 20	$5 \cdot 10^7$	25	$\overline{p}$	LH2	2022 2 years	target spectrometer: tracking, calorimetry
Drell-Yan	Pion PDFs	190	$7 \cdot 10^7$	25	$\pi^\pm$	C/W	2022 1-2 years	
Drell-Yan (RF)	Kaon PDFs & Nucleon TMDs	$\sim$100	10^8	25-50	$K^\pm, \overline{p}$	$NH_3^\uparrow$, C/W	2026 2-3 years	"active absorber", vertex detector
Primakoff (RF)	Kaon polarisa-bility & pion life time	$\sim$100	$5 \cdot 10^6$	> 10	K^-	Ni	non-exclusive 2026 1 year	
Prompt Photons (RF)	Meson gluon PDFs	≥ 100	$5 \cdot 10^6$	10-100	$K^\pm$ $\pi^\pm$	LH2, Ni	non-exclusive 2026 1-2 years	hodoscope
K-induced Spectroscopy (RF)	High-precision strange-meson spectrum	50-100	$5 \cdot 10^6$	25	K^-	LH2	2026 1 year	recoil TOF, forward PID
Vector mesons (RF)	Spin Density Matrix Elements	50-100	$5 \cdot 10^6$	10-100	$K^\pm, \pi^\pm$	from H to Pb	2026 1 year	

we need you!

- a diverse and exciting QCD physics programme is collected for being carried out at a powerful future facility at the M2 beamline of CERN SPS

- further collaborators are currently searched for; signatures are collected until end of 2018

- if interested sign up through our web page:

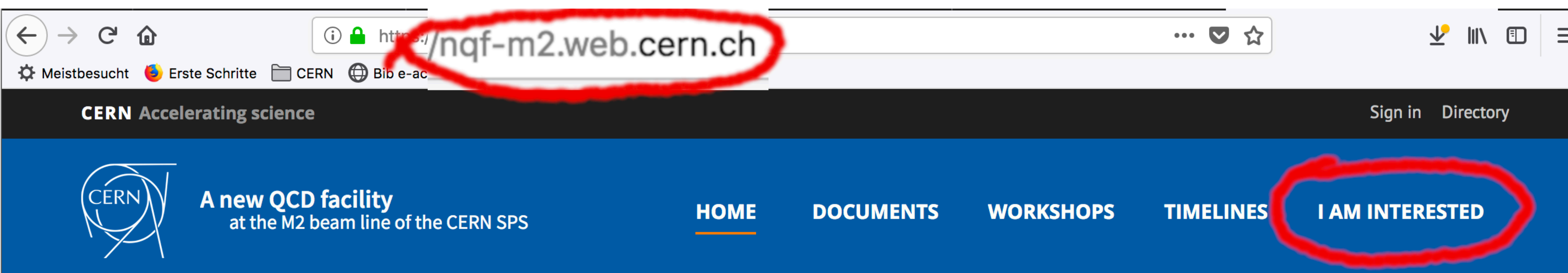

Thank you!

Measurement of chiral dynamics in reactions $\pi^- \gamma^{(*)} \rightarrow \pi^- (n\pi)$

Primakoff data samples:
π^- -nucleus scattering at lowest momentum transfers ➔ $\pi^-\gamma$ reactions
$\pi^- \pi^0$ final state: low-energy part dominated by the chiral anomaly

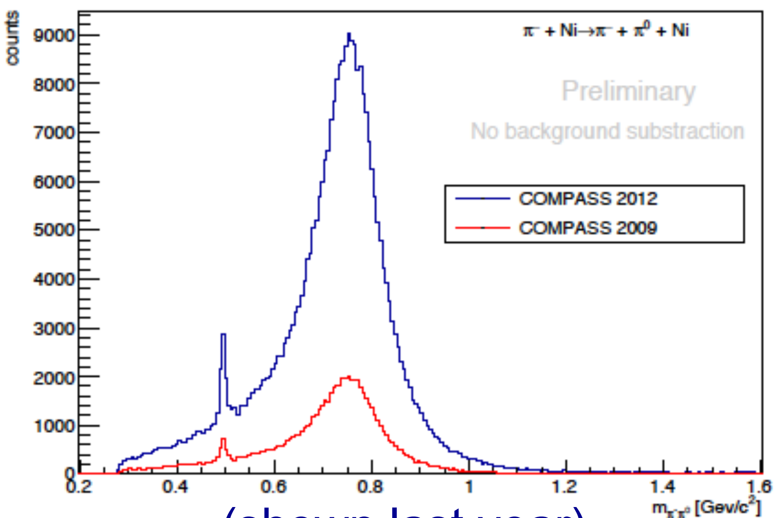

(shown last year)

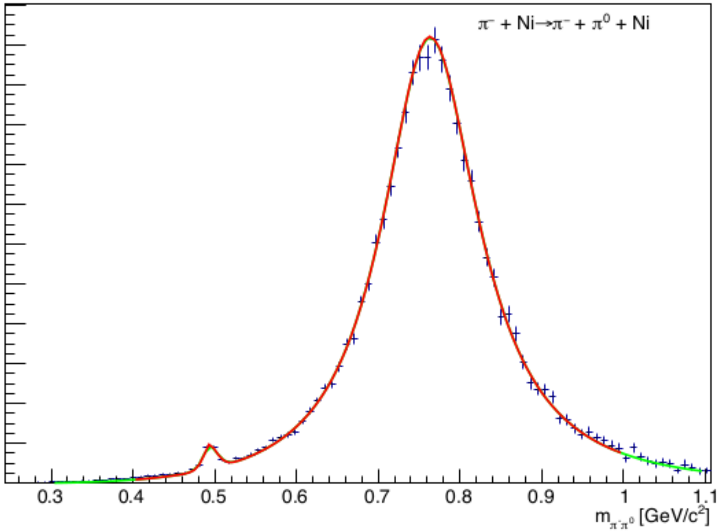

Analysis progress: background subtraction ($\pi^- \pi^0 \pi^0$)
fit to theory (M. Hoferichter *et al*, 2012)
under investigation: luminosity determination

SIDIS transverse & longitudinal

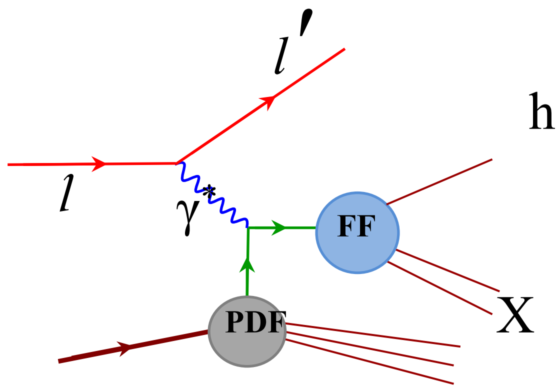

We continue to scrutinize polarised SIDIS data by studying various target-spin-dependent azimuthal asymmetries.
The general expression for polarised SIDIS cross-section contains 6 LO and 6 sub-leading asymmetries

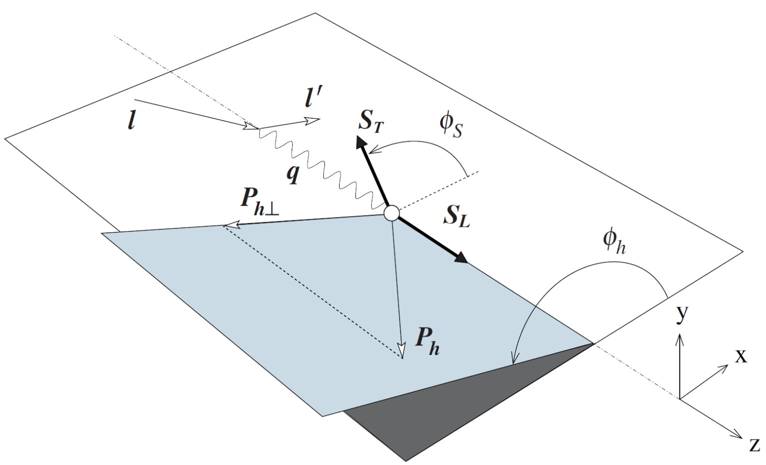

LO LSA/TSA	twist-2: PDF $\otimes$ FF
$A_{UL}^{\sin(2\phi_h)}$	$h_{1L}^{\perp q} \otimes H_{1q}^{\perp h}$
A_{LL}	$g_{1L}^{q} \otimes D_{1q}^{h}$
$A_{UT}^{\sin(\phi_h-\phi_S)}$	$f_{1T}^{\perp q} \otimes D_{1q}^{h}$
$A_{UT}^{\sin(\phi_h+\phi_S-\pi)}$	$h_{1}^{q} \otimes H_{1q}^{\perp h}$
$A_{UT}^{\sin(3\phi_h-\phi_S)}$	$h_{1T}^{\perp q} \otimes H_{1q}^{\perp h}$
$A_{LT}^{\cos(\phi_h-\phi_S)}$	$g_{1T}^{q} \otimes D_{1q}^{h}$

SIDIS longitudinal

longitudinal target-spin-dependent asymmetries (LSA)

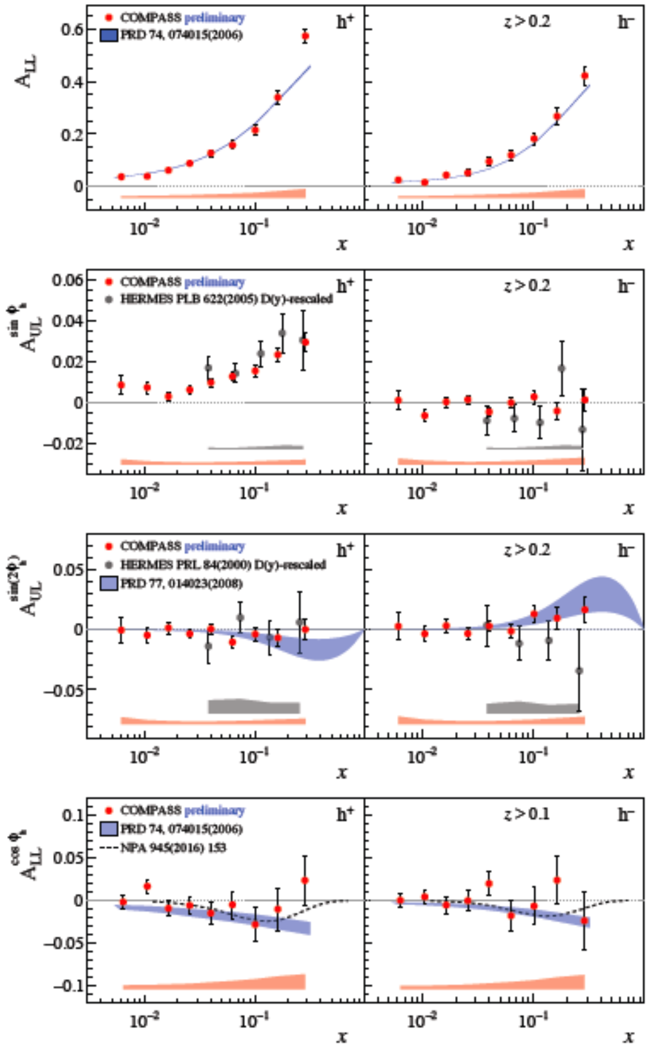

final results for the longitudinally polarised proton target (2007 and 2011 Runs).

error bars: statistical uncertainties
systematic uncertainties indicated by colour bands

compared to the similar studies presented by HERMES and CLAS, our results are characterised by an unprecedented precision, covering a much wider kinematic range

SIDIS transverse
New approach continued: weighted asymmetries

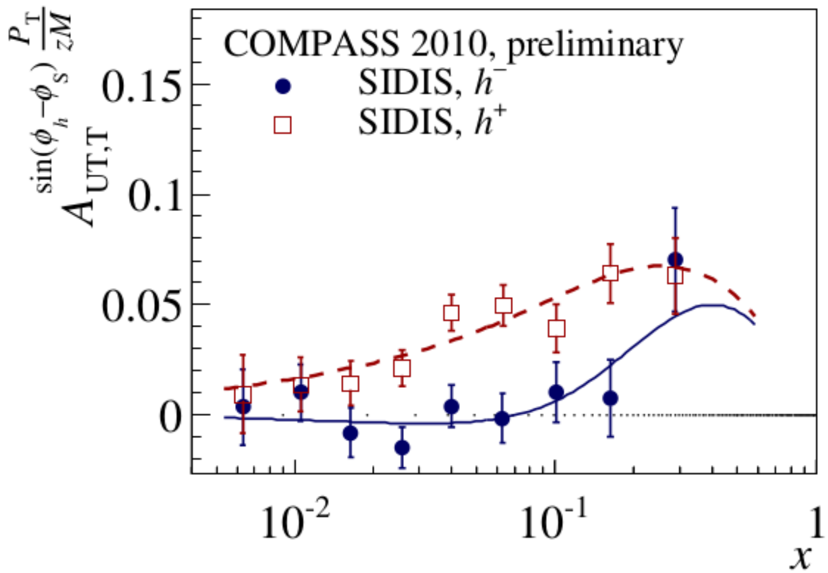

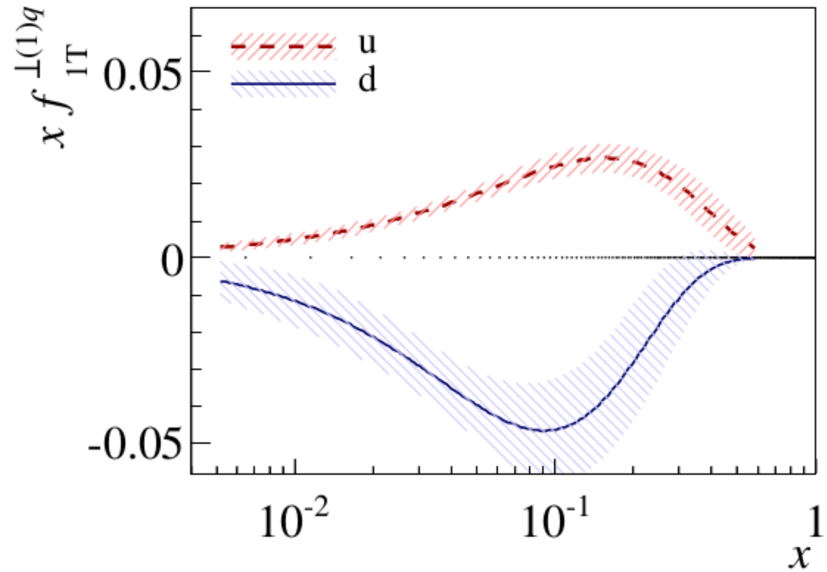

$$A_{Siv}^{(p_T^h/zM)}(x,z) = 2\frac{\sum_q e_q^2 f_{1T}^{\perp(1)\,q}(x)\cdot D_1^q(z)}{\sum_q e_q^2 f_1^q(x)\cdot D_1^q(z)},$$

Important: large statistics, good acceptance.
Allows to extract first moment of Sivers

$$f_{1T}^{\perp(1)}(x,Q^2) = \int d^2k_T \frac{k_T^2}{2M^2} f_{1T}^{\perp}(x,k_T,Q^2).$$

Work in progress:
analogous analysis for weight P_T/M

SIDIS transverse

Proposal for 2021: transverse-deuteron run

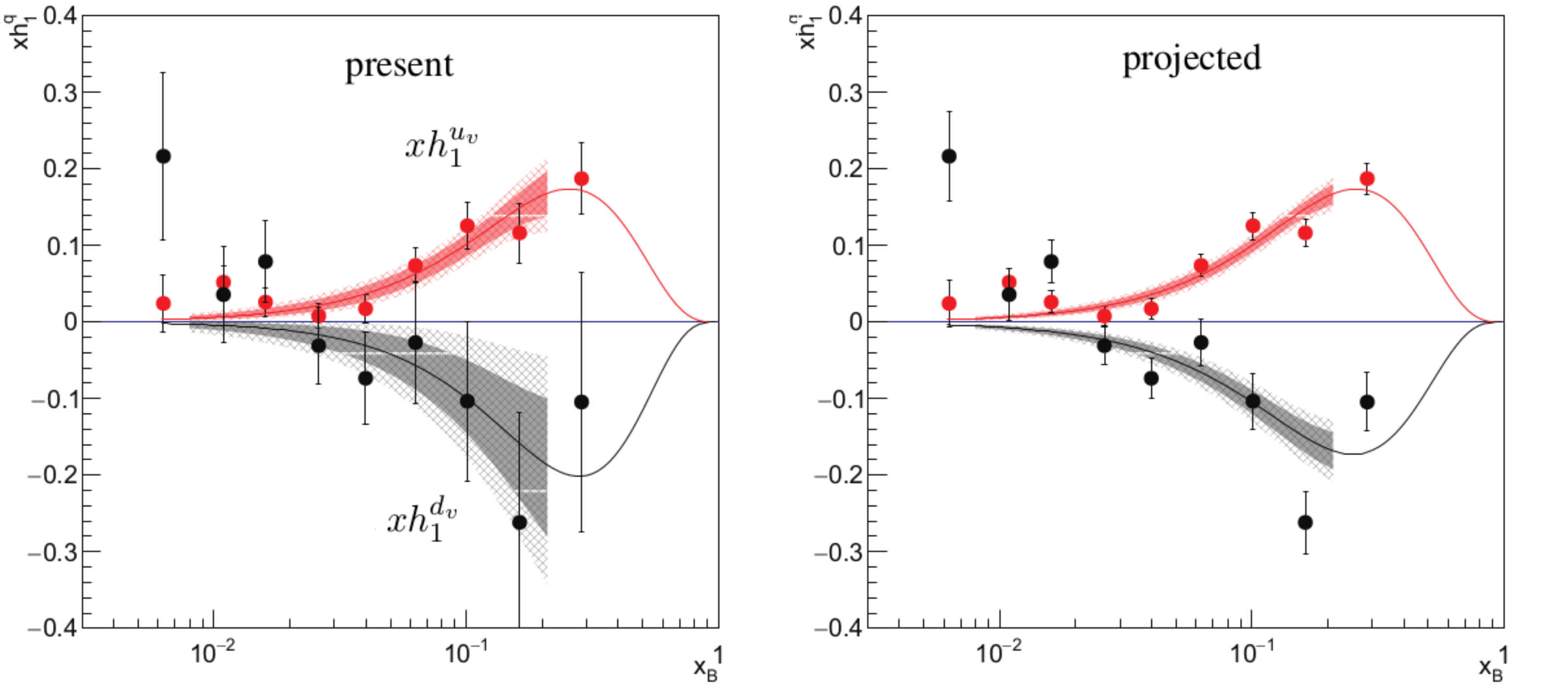

For a precise determination of the Collins functions for u and d, COMPASS is currently lacking an adequate data set with transversely polarised deuteron target.

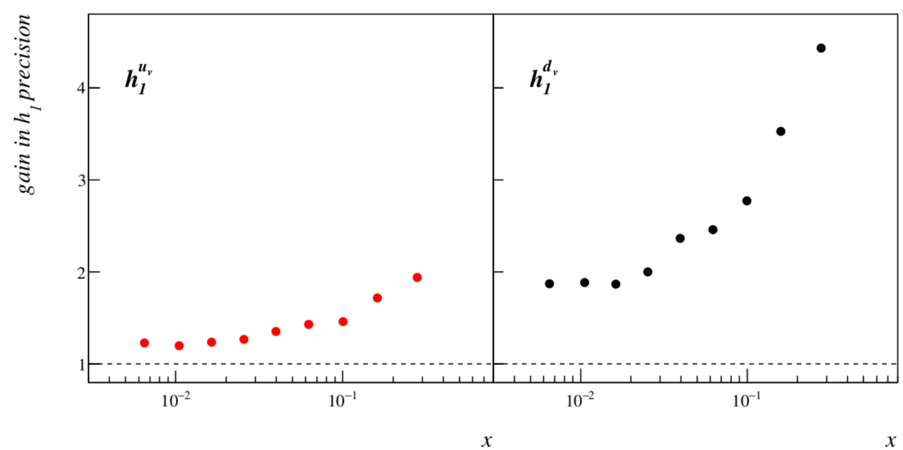

recently recommended by SPSC for approval

SIDIS (kaon) multiplicities

Charged kaon multiplicities (2006 160 GeV ^{6}LiD) – published in PLB 767 (2017) 133
The 3-dimensional data set (*x, y* and *z)* ➔ important input for NLO pQCD analyses of the world data in terms of FFs.

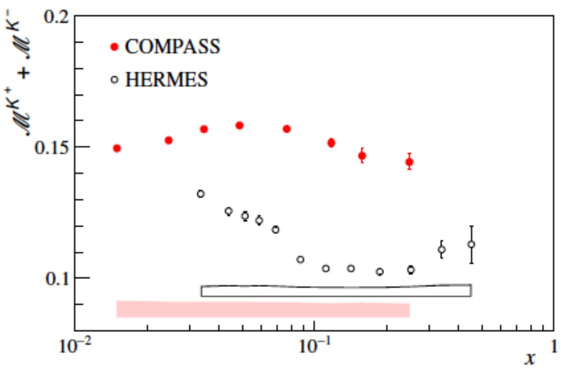

HERMES and COMPASS data are in tension
Can not be explained only by the different Q^2 range

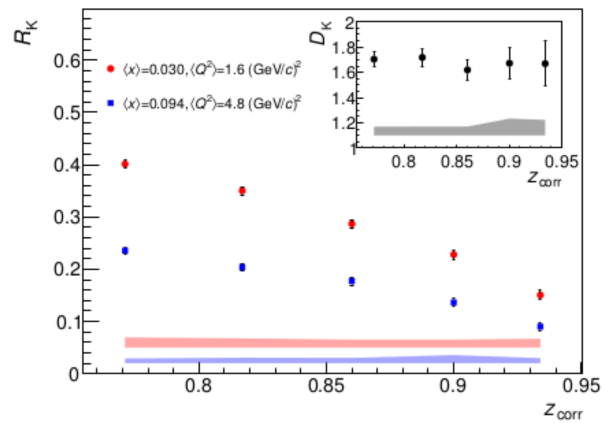

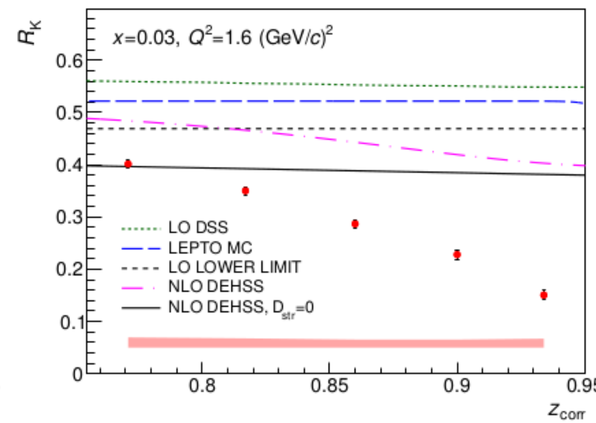

results on the kaon multiplicity ratio K^-/K^+, at high z, 0.75 < z < 1: our data go far beyond the LO upper boundary value of (u+d)/(ū+đ) calculated at x=0.03 using MSTW08L as well as beyond the actual predictions of the ratio using Lund model or LO DSS fit. Recent finding: dependence on M_X

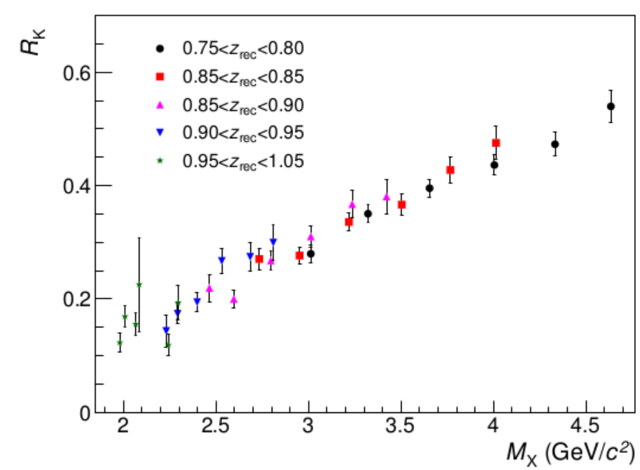

Generalised Parton Distributions – analysis of 2012 data

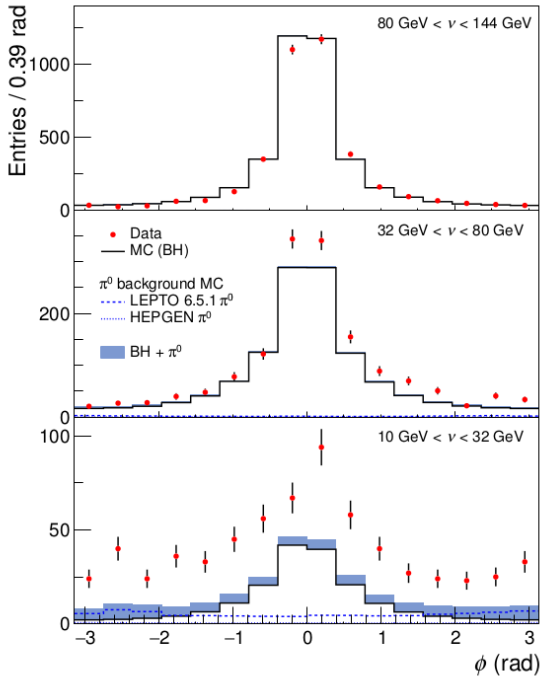

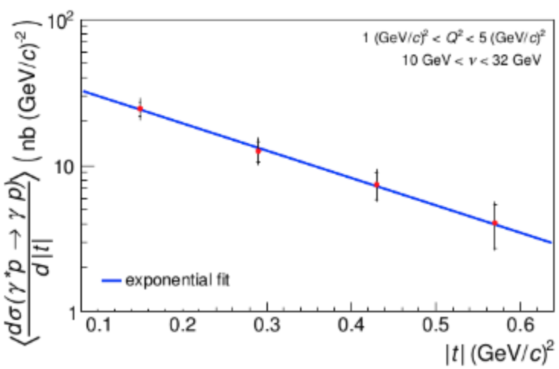

average transverse extension of partons in the proton probed by DVCS (subm. PRL):

$$\sqrt{\langle r_\perp^2 \rangle} = (0.58 \pm 0.04_{\mathrm{stat}} \, {}^{+\,0.01}_{-\,0.02}\big|_{\mathrm{sys}}) \ \mathrm{fm}.$$

SDME via exclusive ω production:

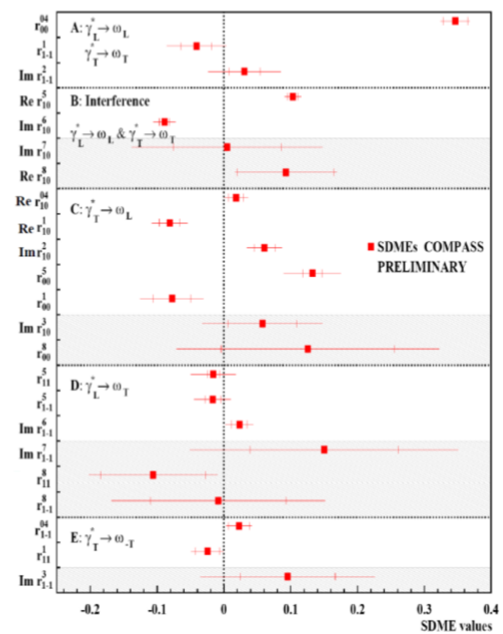

Deeply Virtual Compton Scattering – achieved statistics in 2012 and 2016/17

2016 - 130 days - mainly 2 spills of 4.8 s every 36 s						
	I_{proton} on T6 per spill	I_μ on IonCH per spill	Nb of spills	DAQ life time	Veto life time	Nb of collected muons
μ^+	$100 \cdot 10^{11}$ $70 \cdot 10^{11}$	$7.6 \cdot 10^7$ $5.3 \cdot 10^7$	135527 18592	0.93	0.95	$10.0 \cdot 10^{12}$
μ^-	$100 \cdot 10^{11}$ $70 \cdot 10^{11}$	$6.3 \cdot 10^7$ $4.4 \cdot 10^7$	143848 28255	0.94	0.95	$9.2 \cdot 10^{12}$

2017 - 130 days - mainly 2 spills of 4.8 s every 36 s						
	I_{proton} on T6 per spill	I_μ on IonCH per spill	Nb of spills	DAQ life time	Veto life time	Nb of collected muons
μ^+	$150 \cdot 10^{11}$	$12.5 \cdot 10^7$	168000	0.91	0.93	$17.8 \cdot 10^{12}$
μ^-	$150 \cdot 10^{11}$	$10.5 \cdot 10^7$	195000	0.91	0.93	$17.3 \cdot 10^{12}$

2012 - 30 days - 1 spill of 9.6 s every 48 s						
	I_{proton} on T6 per spill	I_μ on IonCH per spill	Nb of spills	DAQ life time	Veto life time	Nb of used muons
μ^+	$250 \cdot 10^{11}$	$50. \cdot 10^7$		0.84	0.73	$1.87 \cdot 10^{12}$
μ^-	$250 \cdot 10^{11}$	$17.5 \cdot 10^7$		0.94	0.89	$2.33 \cdot 10^{12}$

Assuming data quality in 2016/17 with 80% “good spills”, we collected in 2016/17 about a factor of 10 more statistics compared to 2012

COMPASS Drell-Yan Run 2015 results

PRL **119**, 112002 (2017) PHYSICAL REVIEW LETTERS week ending 15 SEPTEMBER 2017

First Measurement of Transverse-Spin-Dependent Azimuthal Asymmetries in the Drell-Yan Process

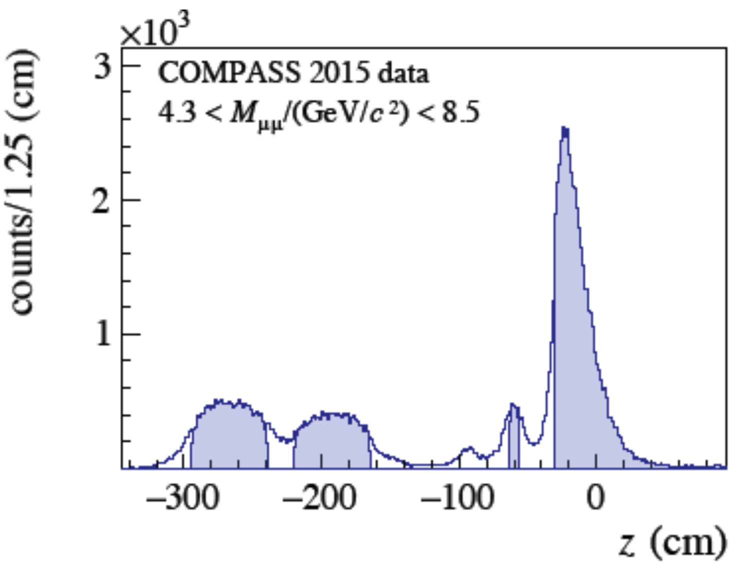

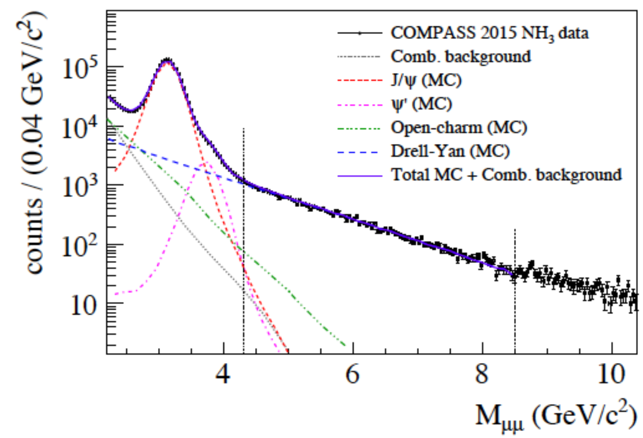

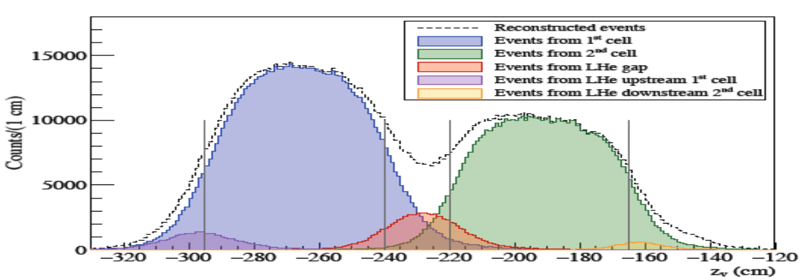

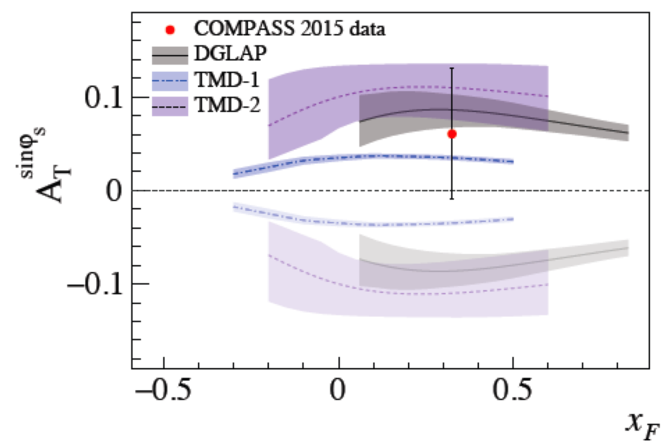

Total number of J/ψ (NH_3) is **~ 1.500.000**

Total number of HM DY (4.3 GeV/c^2 < $M_{\mu\mu}$ < 8.5 GeV/ c^2) (NH_3) is **~35.000**

Central production II

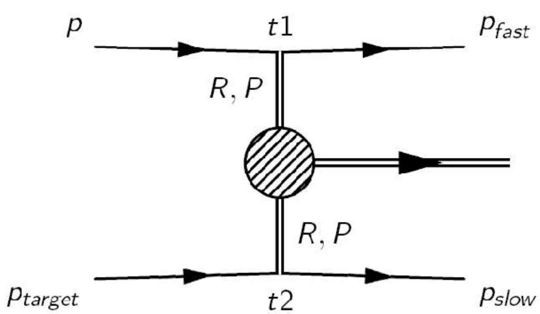

Central production, 2008 and 2009 data.
t_1 t_2 bins, D-wave.
Interestingly, the $f_2(1270)$ signal in the D wave shows a very similar behaviour, which puts strong doubts on the common belief that the $f_2(1270)$ is produced copiously in double-Pomeron processes.

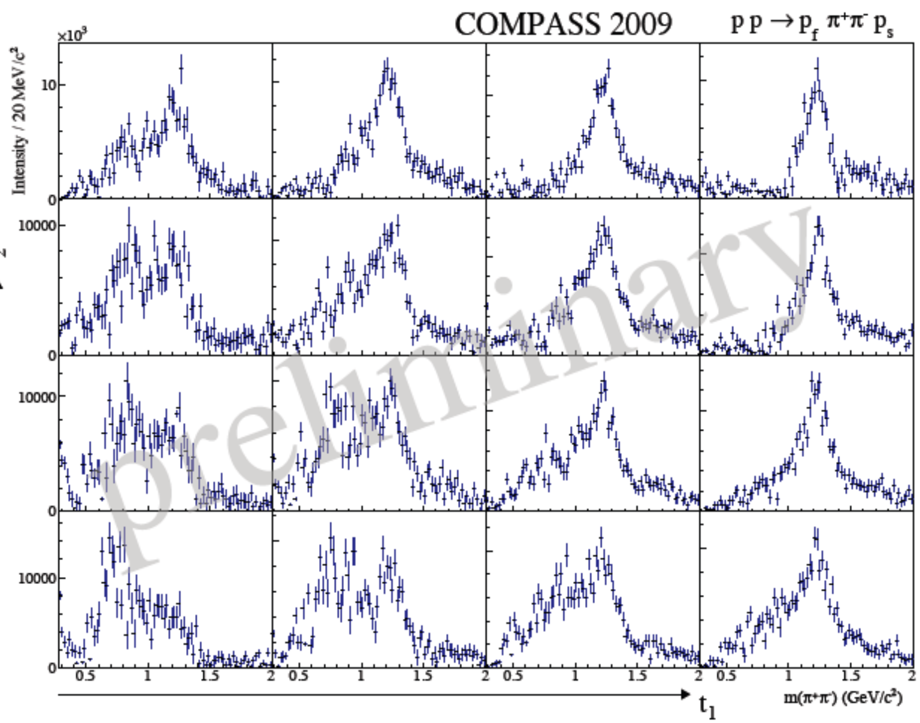

SIDIS transverse&longitudinal I

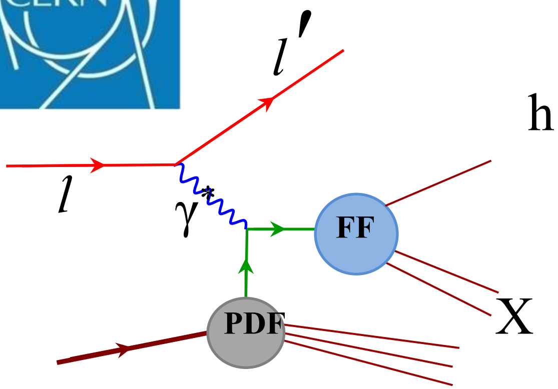

We continue to scrutinize polarised SIDIS data by studying various target spin-dependent azimuthal asymmetries.
General expression for SIDIS cross-section in terms of asym.:

$$
\begin{aligned}
\frac{d\sigma}{dx\,dy\,dz\,d(p_T^h)^2\,d\phi_h\,d\psi} &= 2\left[\frac{\alpha}{xyQ^2}\frac{y^2}{2(1-\varepsilon)}\left(1+\frac{\gamma^2}{2x}\right)\right](F_{UU,T}+\varepsilon F_{UU,L}) \\
&\times\Big\{1+\sqrt{2\varepsilon(1+\varepsilon)}A_{UU}^{\cos\phi_h}\cos\phi_h+\varepsilon A_{UU}^{\cos(2\phi_h)}\cos(2\phi_h)+\lambda\sqrt{2\varepsilon(1-\varepsilon)}A_{LU}^{\sin\phi_h}\sin\phi_h \\
&+S_L\left[\sqrt{2\varepsilon(1+\varepsilon)}A_{UL}^{\sin\phi_h}\sin\phi_h+\varepsilon A_{UL}^{\sin(2\phi_h)}\sin(2\phi_h)\right] \\
&+S_L\lambda\left[\sqrt{1-\varepsilon^2}A_{LL}+\sqrt{2\varepsilon(1-\varepsilon)}A_{LL}^{\cos\phi_h}\cos\phi_h\right] \\
&+S_T\Big[A_{UT}^{\sin(\phi_h-\phi_S)}\sin(\phi_h-\phi_S)+\varepsilon A_{UT}^{\sin(\phi_h+\phi_S)}\sin(\phi_h+\phi_S)+\varepsilon A_{UT}^{\sin(3\phi_h-\phi_S)}\sin(3\phi_h-\phi_S) \\
&\quad+\sqrt{2\varepsilon(1+\varepsilon)}A_{UT}^{\sin\phi_S}\sin\phi_S+\sqrt{2\varepsilon(1+\varepsilon)}A_{UT}^{\sin(2\phi_h-\phi_S)}\sin(2\phi_h-\phi_S)\Big] \\
&+S_T\lambda\Big[\sqrt{\left(1-\varepsilon^2\right)}A_{LT}^{\cos(\phi_h-\phi_S)}\cos(\phi_h-\phi_S) \\
&\quad+\sqrt{2\varepsilon(1-\varepsilon)}A_{LT}^{\cos\phi_S}\cos\phi_S+\sqrt{2\varepsilon(1-\varepsilon)}A_{LT}^{\cos(2\phi_h-\phi_S)}\cos(2\phi_h-\phi_S)\Big]\Big\},
\end{aligned}
$$

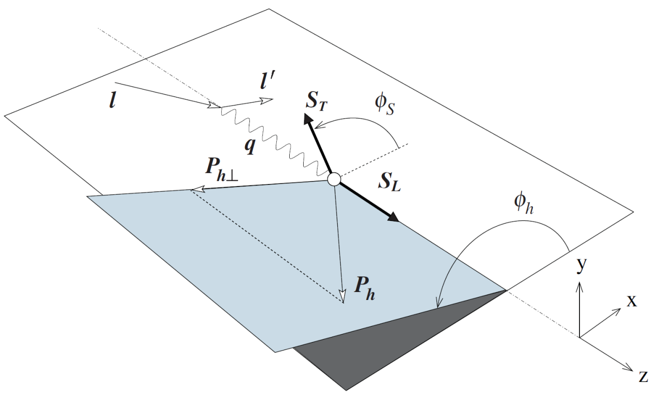

LO LSA/TSA	twist-2: PDF ⊗ FF
$A_{UL}^{\sin(2\phi_h)}$	$h_{1L}^{\perp q}\otimes H_{1q}^{\perp h}$
A_{LL}	$g_{1L}^{q}\otimes D_{1q}^{h}$
$A_{UT}^{\sin(\phi_h-\phi_S)}$	$f_{1T}^{\perp q}\otimes D_{1q}^{h}$
$A_{UT}^{\sin(\phi_h+\phi_S-\pi)}$	$h_{1}^{q}\otimes H_{1q}^{\perp h}$
$A_{UT}^{\sin(3\phi_h-\phi_S)}$	$h_{1T}^{\perp q}\otimes H_{1q}^{\perp h}$
$A_{LT}^{\cos(\phi_h-\phi_S)}$	$g_{1T}^{q}\otimes D_{1q}^{h}$

subleading LSA/TSA	higher-twist PDF ⊗ FF	WWA twist-2: PDF ⊗ FF
$A_{UL}^{\sin(\phi_h)}$	$xh_L^q\otimes H_{1q}^{\perp h}$, $xf_L^{\perp q}\otimes D_{1q}^h$	$h_{1L}^{\perp q}\otimes H_{1q}^{\perp h}$
$A_{LL}^{\cos(\phi_h)}$	$xe_L^q\otimes H_{1q}^{\perp h}$, $xg_L^{\perp q}\otimes D_{1q}^h$	$g_{1L}^q\otimes D_{1q}^h$
$A_{UT}^{\sin(\phi_S)}$	$xf_T^q\otimes D_{1q}^h$, $xh_T^q\otimes H_{1q}^{\perp h}$, $xh_T^{\perp q}\otimes H_{1q}^{\perp h}$	$f_{1T}^{\perp q}\otimes D_{1q}^h$, $h_1^q\otimes H_{1q}^{\perp h}$
$A_{UT}^{\sin(2\phi_h-\phi_S)}$	$xf_T^{\perp q}\otimes D_{1q}^h$, $xh_T^q\otimes H_{1q}^{\perp h}$, $xh_T^{\perp q}\otimes H_{1q}^{\perp h}$	$f_{1T}^{\perp q}\otimes D_{1q}^h$, $h_1^q\otimes H_{1q}^{\perp h}$
$A_{LT}^{\cos(\phi_S)}$	$xg_T^q\otimes D_{1q}^h$, $xe_T^q\otimes H_{1q}^{\perp h}$, $xe_T^{\perp q}\otimes H_{1q}^{\perp h}$	$g_{1T}^q\otimes D_{1q}^h$
$A_{LT}^{\cos(2\phi_h-\phi_S)}$	$xg_T^{\perp q}\otimes D_{1q}^h$, $xe_T^q\otimes H_{1q}^{\perp h}$, $xe_T^{\perp q}\otimes H_{1q}^{\perp h}$	$g_{1T}^q\otimes D_{1q}^h$

SIDIS transverse

New approach continued: weighted asymmetries

Asymmetries obtained by weighting the spin-dependent part of the cross-section with powers of $p^h{}_T$.

Main advantage - convolution integrals becomes products ➔ no parametrization of the unknown transverse momentum dependence of PDFs and FFs is needed.

$$A_{Siv}^{(p_T^h/zM)}(x,z) \; = \; 2\frac{\sum_q e_q^2 f_{1T}^{\perp(1)\,q}(x)\cdot D_1^q(z)}{\sum_q e_q^2 f_1^q(x)\cdot D_1^q(z)},$$

<u>Important</u>: large statistics, good acceptance.

Allows to extract first moment of Sivers

$$f_{1T}^{\perp(1)}(x,Q^2) = \int d^2k_T \frac{k_T^2}{2M^2} f_{1T}^{\perp}(x,k_T,Q^2).$$

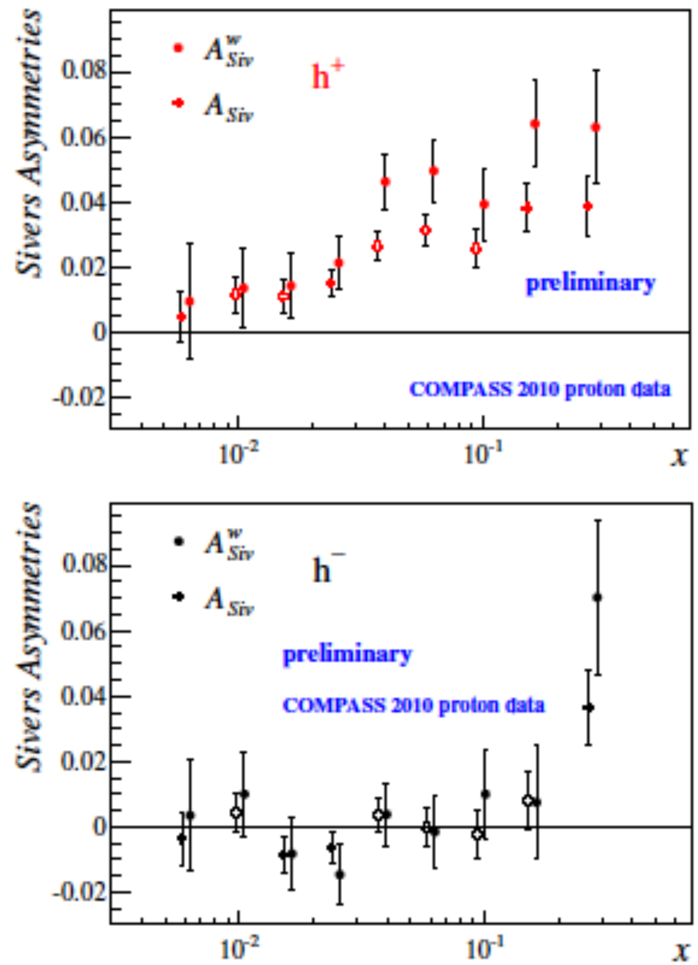

This is a first data on $p^h{}_T$ weighted Sivers asymmetry

SIDIS transverse

Sivers and TSA in the Drell-Yan Q^2 bins

Sivers TMD PDF has a very particular feature - it contributes with opposite sign to SIDIS and DY. It is considered to be an essential prediction of Quantum Chromodynamics (QCD) going to be tested by COMPASS. If Sivers function comparison SIDIS⇐⇒ DY is done at the same Q^2 we drop the uncertainties from the unknown QCD evolution of the Sivers TMD.

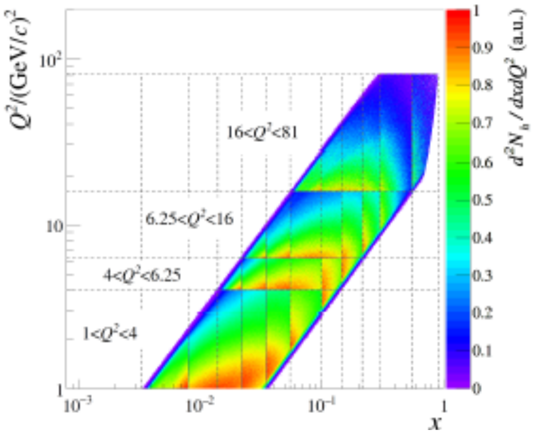

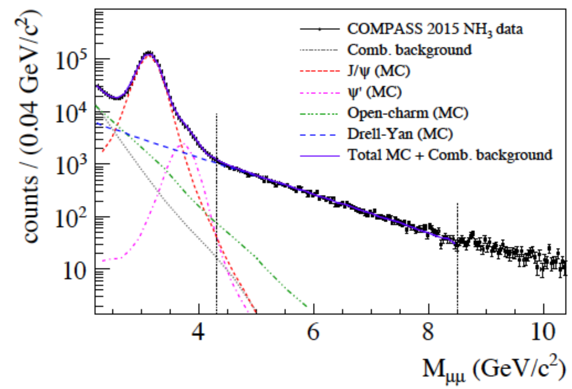

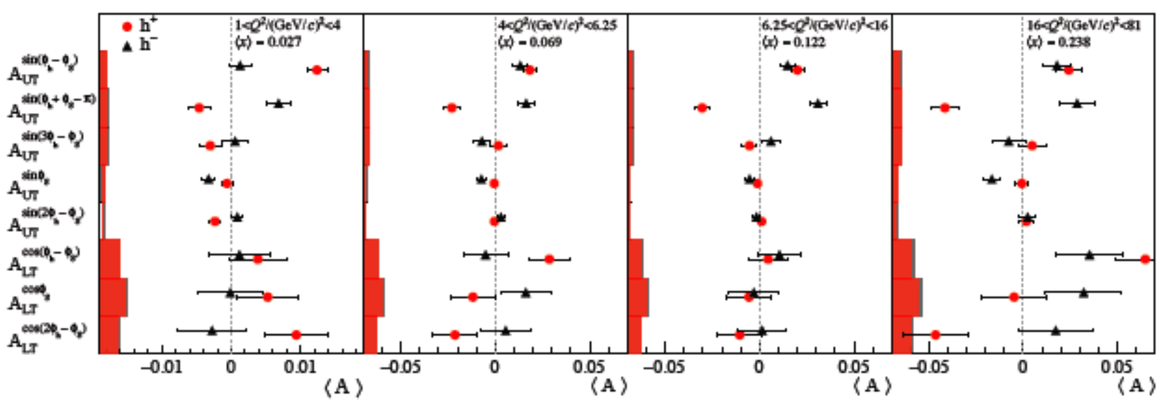

Fig. 2: Mean TSAs in the four DY Q^2-ranges. Systematic uncertainties are shown as error bands next to the vertical axis. For each Q^2-range also the average x-values are given.

(SI)DIS longitudinal I – Final results

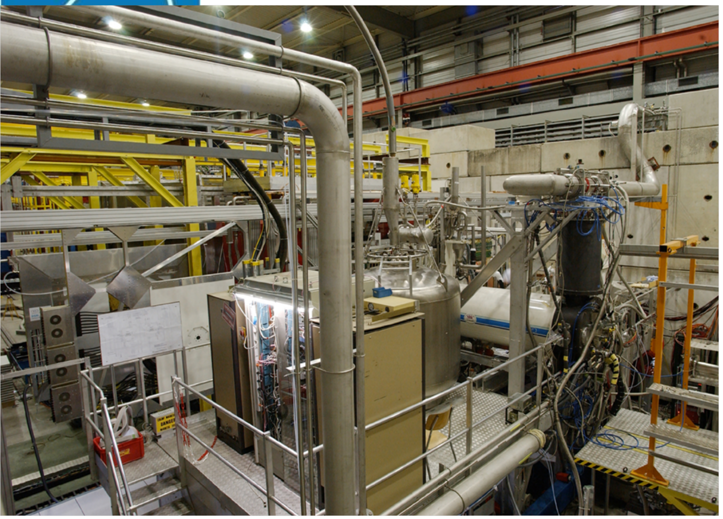

Deuteron g_1^d $Q^2>1$

Published the final COMPASS result for double spin asymmetry A_1^d and longitudinal spin structure function g_1^d (deuteron data set 2002-2004, 2006) PLB 769 (2017) 034. Together with the results on the proton spin structure function g_1^p , these results constitute the COMPASS legacy on the measurements of the g_1 structure function.

All Deuteron data $\Delta g/g$ final result EPJC 77 (2017) 209